Supplementary Information

Multiblock Copolymers toward Segmentation-Driven Morphological Transition

Yi Zheng,[†] Chuang Weng,[†] Cheng Cheng, Jinling Zhao, Rui Yang, Qin Zhang, Mingming Ding, Hong Tan,* and Qiang Fu**

[a] College of Polymer Science and Engineering, State Key Laboratory of Polymer Materials Engineering, Sichuan University, Chengdu 610065, China.

[†]Yi Zheng and Chuang Weng contributed equally to this work.

*Corresponding Author: dmmshx@scu.edu.cn or dmmshx@163.com, hongtan@scu.edu.cn and qiangfu@scu.edu.cn

Materials and Method

Materials

Polyethylene glycol (PEG, MW 2000) was purchased from J&K Scientific Ltd. (Shanghai, China). Cystinedimethyl ester dihydrochloride (L-Cys-OMe·2HCl) was obtained from GL Biochem Ltd. (Shanghai, China). L-lysine ethyl ester diisocyanate (97%) was attained from Nantong Dahong Chemical Co., Ltd. (Jiangsu, China). Triphosgene (99%) was purchased from Adamas (Shanghai, China). Polycaprolactone (PCL, 99%, MW 2000) was purchased from Daicel Chemical Industries, Ltd. (Japan). Methoxy poly (ethylene glycol) (MPEG, MW 2000), Nile red (NR) and rhodamine 6G (R6G) were purchased from TCI Development Co., Ltd. (Tokyo, Japan). ε-caprolactone, stannous octanoate and 3,3'-Diethylthiadicarbocyanine iodide (Cy5) were obtained from Alfa Aesar (China) Chemistry Co., Ltd. (Shanghai China). Dichloromethane (DCM), 1,2-dichloroethane, diethyl ether, triethylamine, tetrahydrofuran (THF), *N,N*-dimethylformamide (DMF), *N,N*-dimethylacetamide (DMAC) and acetone were provided by Chengdu KeLong Chemical Reagent Company (Sichuan, China). Glutathione (GSH) was purchased from Biofroxx (Einhausen, German). Doxorubicin hydrochloride (DOX·HCl) was purchased form Dalian Meilun Biotechnology Co., LTD. (Dalian, China). 3-(4,5-dimethyl-2-thiazolyl)-2,5-diphenyl-2-H-tetrazolium bromide (MTT) and 4',6-diamidino-2-phenylindole (DAPI) were purchased from Sigma (St. Louis, MO, USA). Pyridine was purchased from Lianlong Bohua Medical Chemical Co., Ltd. (Tianjin, China). Buthionine sulphoximine (BSO) was purchased from Shanghai Yuanye Bio-Technology Co., Ltd. (Shanghai, China).

Characterization

All nuclear magnetic resonance spectroscopy (^{1}H NMR, ^{13}C NMR) were recorded on a Bruker Avance III HD 400MHz spectrometer using tetramethylsilane (TMS) as an internal standard and $CDCl_3$ as a solvent at room temperature.

2D nuclear Overhauser effect spectroscopy (NOESY) ^{1}H NMR spectra were measured using an AVANCE III HD spectrometer (400 MHz, JEOL) with a sweep width of 4000 Hz into 1024 data points. The relaxation delay was 2 s and the mixing time was 0.3 s. The number of scans was 4. The concentration of samples was 30 mg mL^{-1}.

Fourier transform infrared (FTIR) spectra were recorded from a Nicolet iS10 spectrometer (Thermo Electron Corporation, U.S.A) from 4000 to 600 cm^{-1} by a transmission mode. The multiblock copolymers were dissolved in chloroform (5%) and dropped onto potassium bromide tablets.

Matrix-assisted laser desorption ionization–time of flight mass spectrometry (MALDI-TOF MS) was performed on an AXIMA Performance (Shimadzu Scientific Instruments; Japan) in the reflector mode and 20 kV acceleration voltage. 2,5-dihydroxy benzoic acid was used as a matrix to facilitate the deposition of samples in the instrument. Sodium or potassium trifluoroacetate was added for ion formation. Samples were prepared from THF solution by mixing matrix (20 mg mL^{-1}), polymers (10 mg mL^{-1}) and salts (10 mg mL^{-1}) in a ratio of 10:1:1. The number-average molecular weights (M_n) of the polymeric samples were determined in the linear mode.

The molecule weight and molecular weight distribution were determined by gel permeation chromatography (GPC) with an HLC-8320 (TOSOH Corporation, Japan) at room temperature using THF as an eluent. The molecular weights were calibrated against polystyrene (PS) standards. The sample concentration was 2 mg mL^{-1} and the flow rate was 1.0 mL min^{-1}.

The morphology of samples was observed using a transmission electron microscope (TEM), which was acquired on a model H-600-4 (Hitachi, Ltd., Japan) operated at an accelerating voltage of 75 KV. TEM grids were prepared by depositing a diluted suspension of sample onto a copper grid with staining with 1% (w/v) phosphotungstic acid for 3 min, the excessive solution was blotted away and air dried before imaging.

Fluorescence measurement was conducted on an F-4600 FL spectrophotometer (Hitachi, Ltd., Japan). For pyrene fluorescence, the excitation spectra were collected from 206 nm to 406 nm at an emission wavelength (λ_{em}) of 372 nm, the emission spectra were collected from 350nm to 550nm at an excitation wavelength (λ_{ex}) of 331nm. For R6G fluorescence, the emission spectra were collected from 535 nm to 700 nm at a λ_{ex} of 526 nm. For NR fluorescence, the emission spectra were collected from 545 nm to 800 nm at a λ_{ex} of 543 nm. For Forster resonance energy transfer (FRET) measurements, the emission spectra were collected from 500 nm to 800 nm at a λ_{ex} of 480 nm.

Circular dichroism (CD) was measured on a J-1500-150 spectrometer (JASCO Corporation, Japan) at room temperature in the range of 190 nm to 300 nm. A quartz cell containing a light path of 1 mm was used to place the sample solution. The mean

residue molar ellipticity of polymers was calculated on the basis of determined apparent ellipticity by the following formulas: ellipticity ([θ] in deg cm^2 $dmol^{-1}$) = (millidegrees × mean residue weight)/ (path length in millimeters × concentrations of polypeptide in mg mL^{-1}).[S1, S2]

The size and zeta potential of polymer assemblies were obtained on a Zetasizer Nano ZS instrument (Malvern Instruments Ltd., UK) at room temperature at an angle of 90°. The relevant data were presented as mean ± standard deviation (SD) based on triplicate independent experiments.

Static light scattering (SLS) and dynamic light scattering (DLS) were carried out on a Spectra Physics Millennia-II diode laser and a Brookhaven Instruments BI-200SM goniometer with a BI-9000 correlator. All samples were prepared from aqueous polymer solutions and studied at 25 °C. The solutions with a concentration of 50 μg mL^{-1} were purified by passing through a 0.45 μm Millipore filter (PVDF). The scattered light was a 532 nm laser from a Spectra Physics Millennia II laser. The detection angle ranged from 30° to 150°, with 15° increments between angles. Three repeat measurements of scattered light intensity were taken at each angle and concentration. CONTIN analyses were used for the extraction of R_H data from DLS measurements. The R_G data were obtained from SLS measurements. Finally, the characteristic parameter (ρ) was calculated from the ratio of R_G / R_H.

Small-angle X-ray scattering (SAXS) experiments were performed under vacuum at room temperature on a Xeuss 2.0 instrument (Xenocs Corporation, France) with a Dectris Pilatus detector and Cu-Kα radiation (λ = 1.54 Å) and at 50 kV and 0.6 mA. For

the measurement of assemblies, an aqueous dispersion of polypeptide (10 mg mL^{-1}) was mounted into a quartz capillary with 1.5 mm diameter and sealed with parafilm to prevent solvent evaporation. Data were collected using a Dectris Pilatus detector. The sample-to-detector distance was 2.5 m, and the exposure time was 30 min. All the samples were analyzed in the q range of 0.01 to 0.2 $Å^{-1}$, and the length of scattering vector q was defined as:

$$q = (4\pi\sin\theta) / \lambda$$
$$= 2\pi / d \quad \text{(S1)}$$

where λ is the wavelength of the X-ray, and θ is half of the scattering angle. The SAXS data were reduced to remove the solvent background from the acquired sample scattering profiles using a Foxtrot 3.2.7 software, and further analyzed by fitting to model expressions using a SasView 5.0 software package.

Differential scanning calorimetric (DSC) was carried out on a TAQ20 instrument. 3-5 mg of polymer powders were enclosed in an Al_2O_3 crucible, heated from room temperature to 80 °C at a rate of 10 °C min^{-1}, and then cooled to -80 °C at the same rate. After holding the temperature for 3 min, the samples were heated to 80 °C again at the same rate. This measurement was carried out in an atmosphere of flowing nitrogen gas. Super-sensitive DSC measurement was performed using a Microcal VP-DSC differential scanning calorimeter (Microcal) at a heating rate of 1.5 °C min^{-1} in the temperature range of 20 to 80 °C. The polymeric assemblies were prepared in an aqueous solution (1 mg mL^{-1}) for analysis. Although the obtained C_p values were

relatively low due to the low concentrations of polymeric assemblies, significant difference between P2 and P4 samples could be observed from Fig.S10.

The X-ray diffraction (XRD) patterns were used to acquire the information on crystallography and measured on a Phliphs X' Pert PRO, XL-30 diffractometer with Cu4Kα radiation. The XRD data over the 5-60° range were collected.

Synthesis of L-Cystine Dimethyl Ester Diisocyanate (CDI)

The synthetic route of CDI was shown in Scheme S1. In brief, Cys·OMe·2HCl (10.2 g) was dissolved in anhydrous dichloromethane (DCM) and pyridine under dry argon. Then triphosgene (7.7 g) was dissolved in DCM and added dropwise into the reaction system for 5 h of reaction at -5 °C. Afterward, the reaction mixture was washed with cold HCl solution (0.5 M) and deionized water for three times. The organic phase was collected and dried with anhydrous Na_2SO_4 overnight. Then the solution was filtered and condensed under reduced pressure. The crude products were purified by recrystallization from dried THF/*n*-hexane to obtain a white needle-shaped solid (75.0 % yield). ^{1}H NMR (400 MHz, $CDCl_3$, TMS, δ): 4.40 (dd, 1H, =N-CH), 3.85 (s, 3H, -O-CH_3), 3.21 (dd, 1H, -S-CH_2), 3.07 (dd, 1H, -S-CH_2). ^{13}C NMR (400 MHz, $CDCl_3$, δ): 169.6, 127.56, 56.58, 53.63, 42.97. FTIR (cm^{-1}): 2260 (s, *v* N=C=O),1750 (s, *v* C=O), 1300 (s, *v* C-O-C). MS-ESI (m/z): $[M+Na]^+$ caled: 320.01; observed: 320.183.

Synthesis of Multiblock Copolymers with Different Block Numbers (P1-P4)

Typically, multiblock copolymers with different block numbers were prepared *via* a facile one-step polymerization (Scheme S2). Briefly, PEG (3.0 g) and PCL (3.0 g) were dissolved in anhydrous dichloroethane (DCE, 60 mL) under dry argon. Then, CDI

(0.5 g / 0.84 g / 1.01 g) and stannous octoate (0.1%) were added into the reaction systems. The reaction was performed at 60 °C for 24 h, and continued at 80 °C for additional 24 h. Then the solution mixture was condensed by evaporation and precipitated in ice diethyl ether for three times to give a white solid (72% yield). Multiblock copolymers with different block sequences and linkers were synthesized according to Scheme S3 and S4.

To synthesize diblock copolymer P1 as a control, MPEG-PCL was prepared through ring opening polymerization of ε-caprolactone (ε-CL) initiated by MPEG (Scheme S5). Briefly, MPEG (2.0 g) was dissolved in DCE under dry argon. Then, 1.8 mL of ε-CL and 5.5 μL of stannous octoate were added. After reaction for 24 h at 115 °C, the solution mixture was condensed by evaporation and precipitated in ice mixture solution of diethyl ether and methanol for three times to give a white solid (82% yield).

The structures of products were characterized with FTIR, ^{1}H NMR, ^{13}C NMR, GPC, and MALDI-TOF. The FTIR spectra of multiblock copolymers are depicted in Figure S4. The characteristic peak of -N=C=O group (2270 cm^{-1}) disappears, indicating that the isocyanate groups in CDI have been completely reacted with PCL and PEG. Furthermore, a broad stretching band observed at 3300-3360 cm^{-1} is mainly attributed to the N-H stretching vibration,[S3-S5] while the stretching band in the 1600-1800 cm^{-1} region is due to the absorption of ester carbonyl groups of PCL,[S6, S7] free and hydrogen-bonded carbonyl of urethane groups.[S4, S8]

Fig. S2 presents the ^{1}H NMR spectra of multiblock copolymers. The peaks at 4.05 (-C***H***$_2$O-), 2.30 (-C***H***$_2$COO-), 1.67 (-C***H***$_2$CH$_2$C***H***$_2$-) and 1.38 (-CH$_2$C***H***$_2$CH$_2$-) ppm are

assigned to the methylene protons of PCL segment. The peak at 3.65 ppm (-C***H***$_2$C***H***$_2$O-) is ascribed to the methylene groups of PEG block. The chemical shifts of methylene and methyl groups of CDI residue are at 3.16 and 3.77 ppm (-C***H***$_2$-S-, C***H***$_3$O-), respectively. Moreover, the active protons in urethane groups were observed at 5.55-6.28 ppm (-N***H***COO-). In ^{13}C NMR spectra (Fig.S3), the ^{13}C resonance signals at 24.5, 25.5, 28, 34, 64, and 173.5 ppm are assigned to the six carbons of PCL unit. The peak at 70.5 ppm is attributed to PEG segment. The peaks at 53 and 173.5 ppm are derived from CDI. In addition, the actual composition of multiblock copolymers was calculated from the integral area of the ^{1}H NMR peaks at 3.77 ppm (CDI), 1.67 ppm (PCL) and 3.65 ppm (PEG). Accordingly, the PCL/PEG molar ratios were calculated to be 1.01, 0.97, 0.95 and 1.01, respectively, for P1, P2, P3 and P4. The molecular weights of multiblock copolymers were also determined integration of ^{1}H NMR peaks at 3.77 ppm (CDI), 1.67 ppm (PCL) and 3.65 ppm (PEG). The results are in good agreement with MALDI-TOF MS analysis (Table 1), which provide the absolute number average molecular weight of copolymers. Therefore, the block numbers of polymers were estimated to be 2, 4, 10, 20 for P1, P2, P3 and P4, respectively. GPC diagrams confirm the success of block number control, where the weight average molecular weights are in the range of 7800 to 48100, with narrow molecular weight distributions (Fig.S3, Table 1).

Synthesis of Multiblock Copolymers with Different Block Sequence (P4-D)

To understand the effect of block sequences on segmentation-driven shape transition, we synthesized a control copolymer with different block arrangement (P4-

D), where PCL and PEG blocks were incorporated separately, resulting in the formation of PCL- and PEG-rich domains (Scheme S3). In brief, PEG (3.0 g) and PCL (3.0 g) were dissolved in 30 mL DCE separately in two flasks. Each of the flasks was added with 0.44 g of CDI and 0.1% stannous octoate under a dry argon atmosphere for 24 h of reaction at 70°C. Then the two reaction systems were mixed and added with an additional 0.22 g of CDI. The reaction was continued for 24 h at 80 °C, and the solution mixture was condensed by evaporation and precipitated in ice mixture solution of diethyl ether and methanol for three times to give white solid.

Figure S11 presents the ^{1}H NMR spectra of multiblock copolymers. The peaks at 4.05 (-C***H***$_2$O-), 2.30 (-C***H***$_2$COO-), 1.64 (-C***H***$_2$CH$_2$C***H***$_2$-) and 1.38 (-CH$_2$C***H***$_2$CH$_2$-) ppm are assigned to the methylene protons of PCL segment. The peak at 3.64 ppm (-C***H***$_2$C***H***$_2$O-) is ascribed to the methylene groups of PEG block. The chemical shifts of methylene and methyl groups of CDI residue are at 3.16 and 3.78 ppm (-C***H***$_2$-S-, C***H***$_3$O-), respectively. Moreover, the active protons in urethane groups were observed at 5.55-6.28 ppm (-N***H***COO-). The actual composition of multiblock copolymers was calculated from the integral area of the ^{1}H NMR peaks at 3.78 ppm (CDI), 1.64 ppm (PCL) and 3.64 ppm (PEG). Accordingly, the PCL/PEG molar ratios were calculated to be 1.08. GPC diagram indicates that the weight average molecular weight of P4-D is 56429 g mol^{-1}, with narrow molecular weight distributions (PDI 1.37, Figure S12).

To further prove the success of sequence regulation, lipase enzymatic degradation of P4 and P4-D were carried out. The lipase enzyme selectively decomposes PCL components, allowing for a facile analysis of polymeric structure by examining the PEG

residues. In briefly, P4 and P4-D solutions were cultured with 0.2 mg mL^{-1} of lipase PS. The change of molecular weights was detected by GPC. As shown Fig.S12, the molecular weights of P4 and P4-D both decrease significantly after enzymatic treatment, indicating that the copolymers were degraded by lipase PS. Encouragingly, the molecular weight of P4 after enzymatic degradation is comparable to that of PEG monomer. This result verifies that the PEG blocks are divided by PCL segments, *i.e.*, the multiblock copolymer possesses a nearly alternating hydrophobic and hydrophilic architecture. In contrast, the molecular weight of P4-D after enzymatic degradation is several times higher than that of PEG, implying the presence of PEG-rich domains in the polymer backbone, where multiple PEG blocks were linked by CDI. The enzymatic degradation experiment confirms the different block sequences of P4 and P4-D.

Synthesis of Multiblock Copolymers with Different Linker (P4-L)

To investigate the effect of coupling agent structure on the self-assembly of multiblock copolymers, another control polymer P4-L with different linker was synthesized using a commercial L-lysine ethyl ester diisocyanate (LDI) as a coupling agent instead of CDI (Scheme S4). Briefly, PEG (3.0 g) and PCL (3.0 g) were dissolved in anhydrous DCE (60 mL) under dry argon. Then, LDI (0.34 g) and stannous octoate (0.1%) were added into the reaction systems. The reaction was performed at 60 °C for 24 h, and continued at 80 °C for additional 24 h. Then the solution mixture was condensed by evaporation and precipitated in ice diethyl ether for three times to give white solid.

The obtained P4-L was characterized by ^{1}H NMR and GPC. As shown in Fig. S22, the characteristic peaks of PEG and PCL were clearly detected in $CDCl_3$. The peaks at 4.05 (-C***H***$_2$O-), 2.31 (-C***H***$_2$COO-), 1.64 (-C***H***$_2$CH$_2$C***H***$_2$-) and 1.38 (-CH$_2$C***H***$_2$CH$_2$-) ppm are assigned to the methylene protons of PCL segment. The peak at 3.65 ppm (-C***H***$_2$C***H***$_2$O-) is ascribed to the methylene groups of PEG block. The chemical shifts of methylene and methyl protons in ethoxyl group of LDI groups are at 4.26 (-C***H***$_2$OCO-) and 1.26 (-C***H***$_3$) ppm. Moreover, the active protons in urethane groups were observed at 5.55-6.28 ppm (-N***H***COO-). The ratio of PEG/PCL was 0.96 and the block number was 23 as calculated by integration of the characteristic peaks of PEG and PCL in ^{1}H NMR spectra. GPC analysis indicates that the molecular weight of P4-L was 51707 g mol^{-1} with a narrow distribution (PDI 1.27, Fig.S23). These results indicate that multiblock copolymer with different linker was synthesized successfully.

Self-Assembly of Multiblock Copolymers

The assemblies of block copolymers were prepared using a dialysis method. Briefly, solutions of polymers (10 mg) in 1 mL of DMAC were added dropwise to 9 mL of deionized water with quickly stirring. Then the solutions were transferred into a dialysis bag (MWCO 3500) and dialyzed against deionized water for 3 d, changing the external water once 3 h. Finally, the solutions were centrifugalized for 15 min at 3000 r min^{-1} and filtered through a 0.45 μm pore-sized syringe filter (Millipore, Carrigtwohill, Co. Cork, Ireland).

Pyrene Fluorescence Probe Study

The critical aggregation concentration (CAC) values of polymer assemblies were measured by a fluorescence method using pyrene as a probe.[S9, S10] Briefly, 20 μL of acetone solutions of pyrene (5.0×10^{-6} mol L^{-1}) were transferred into a series of vials and acetone was evaporated under argon flow. Then 2 mL of polymer self-assemblies with different concentrations were added into the vials and ultrasonated for 2 h. The steady-state fluorescence excitation spectra were recorded on an F-4600 FL spectrophotometer at λ_{em} of 372 nm, with bandwidths of 5 nm for excitation and 5 nm for emission. The intensity ratio of the peak at 337.7 nm to that at 334.6 nm ($I_{337.7}$ / $I_{334.6}$) from the excitation spectra and that between the first peak and third peak (I_1 / I_3) from emission spectra were plotted against the log of the polymer concentrations. The CAC values were obtained from the intersection of the two trend lines shown in Figure S5.

Determination of Aggregation Number (N_{agg})

The weight-average molecular weights of polymeric assemblies were measured by SLS using the Debye plot. The aggregation numbers of polymeric assemblies were calculated by eq S2:

$$\text{Aggregation Number} = \frac{M_{w,aggregate}}{M_{w,block\ copoolymer}} \quad \text{(S2)}$$

where $M_{w,\ aggregate}$ is the weight-average molecular weight of polymeric assemblies estimated by SLS and $M_{w,\ block\ copolymer}$ is the sum of weight-average molecular weight of polymer estimated by integration of NMR peaks.[S11]

R6G Encapsulation Study

A solution of R6G in deionized water (200 μL, 0.2 mg mL^{-1}) was added dropwise into 2 mL of assembled solutions prepared from multiblock copolymers (0.2 mg mL^{-1}) with constant stirring for 0.5 h. After that, the solutions were ultrasonated for 2 h. The solution was transferred to a dialysis bag (MWCO 3500) and dialyzed against water for 24 h, changing the water every 3 h. The solutions were measured using UV-Vis spectrometer and the concentration of free R6G in water was adjusted so that the UV-Vis absorption matches that of R6G encapsulated in assemblies. The fluorescence emission spectra of R6G in water and assembled solutions were recorded on an F-4600 FL spectrophotometer (Hitachi, Ltd., Japan) at a λ_{ex} of 526 nm.

For fluorescence self-quenching test, R6G dissolved in water and encapsulated in assembled solutions were added in a black 96-well plate with same concentration as measured by UV-Vis spectrometer. The plate was imaged using an IVIS Lumina Series III imager (PerkinElmer, MA, USA). The excitation filter and emission filter are 520 nm and 570 nm, respectively, and the field of view is 10 cm. In addition, the fluorescence intensity decay of R6G was determined on an IBH TEMPRO-01 (Horiba, Japan). The obtained fluorescence decay $N(t)$ is a convolution of the sample's intrinsic fluorescence decay $I(t)$ with the instrument response function (IRF) ($L(t)$). For a sample with a multi-exponential lifetime, the fluorescence signal $N(t)$ is represented as

$$N(t) = L(t) \otimes I(t)$$
$$= L(t) \otimes \sum A_i \exp(-t/\tau_i) \quad \text{(S3)}$$

Where τ_i is lifetime with corresponding intensity coefficients A_i. Fluorescence lifetime data were analyzed using DAS6 software. The luminescence intensity $I(t)$ of R6G was well modelled by the sum of two exponential decay components, i.e.,

$$I(t) = \sum A_i \exp(-t/\tau_i) \quad \text{(S4)}$$

The average lifetime, τ_{ave}, was then calculated using the following equation:

$$\tau_{ave} = \sum A_i \tau_i / \sum A_i \quad \text{(S5)}$$

The fluorescence decay profiles of R6G dissolved in water and that encapsulated in multiblock copolymers assemblies were shown in Figure S7, and the calculated lifetime values were listed in Table S2. It was found that the lifetime values of R6G in P1, P2 and P3 assemblies are the same as that in water (3.9 ns), while the lifetime decreases to 3.34 ns for R6G entrapped in P4 assemblies. Such a decrease of fluorescence lifetime indicative of a tracer–tracer collisional self-quenching.[S12-S15] Interestingly, the fluorescence decay curve of R6G in the presence of P4 assemblies fits a double exponential function, suggesting that the dye was present in a double environments. In particular, a lifetime of 1.009 ns comprised 20% of the decay function was derived from R6G encapsulated in P4 assemblies, while another lifetime of 3.9 ns comprised 80% of the decay function was attributed to the free dye dissolved in water (Table S2). This result implies that the leakage of some dye molecules from vesicles had occurred before fluorescence measurement.[S12] As expected, the fluorescence decay curves of R6G in the presence of other multiblock polymer assemblies fit a single exponential function.

NR Loading Study

NR as a model hydrophobic cargo was loaded into multiblock copolymer (P1-P4 and P4-L) assemblies. In brief, a solution of NR in acetone (200 μL, 0.2 mg mL^{-1}) was added dropwise into 2 mL of assembled solutions prepared from multiblock copolymers (0.2 mg mL^{-1}) with constant stirring for 24 h. Finally, the solutions were centrifugalized for 15 min at 3000 r min^{-1} and filtered through a 0.45 μm pore-sized syringe filter (Millipore, Carrigtwohill, Co. Cork, Ireland).

R6G and NR Encapsulation Study

To verify the assembled structure, a solution of R6G in water (100 μL, 0.1 mg mL^{-1}) and NR (100 μL, 0.1 mg mL^{-1}) in acetone were added dropwise into 1 mL of assembled solutions prepared from MBCs (1 mg mL^{-1}). The solution was stirred for 30 min, transferred into a dialysis bag (MWCO 3500) and dialyzed against deionized water for 12 h to remove free dyes and acetone. Finally, the solution was centrifugalized for 10 min at 3000 r min^{-1} and filtered through a 0.45 μm pore-sized syringe filter (Millipore, Carrigtwohill, Co. Cork, Ireland). The resulting fluorescent-labeled assemblies were dropped on a glass slide, air-dried and mounted with 10% glycerol solution, then imaged by a confocal laser scanning microscope (CLSM, Nikon A1 RMP+, Nikon, Japan) with an objective of 100× magnification and 1.49 NA.

Urea Addition Experiment

To study the impact of hydrogen-bonding on the self-assembled morphologies, the NR-loaded multiblock copolymer dispersions in aqueous solutions were added with 7 M urea, a strong breaker of hydrogen bonding.[S16, S17] The change in fluorescence intensity of NR probe was monitored with an F-4600 FL spectrophotometer (Hitachi,

Ltd., Japan) at a λ_{ex} of 543 nm. For comparation, free NR solutions in methanol was also treated with urea and analyzed to investigate the effect of urea addition on NR fluorescence.

As can be seen from Figure S19, with the addition of urea, the fluorescence intensity of NR decreases slightly for all the samples to a same extent, and then no further change occurs over time. We suspected that the initial decrease of fluorescence intensity is attributed to the impact of urea on NR itself. To test this hypothesis, we added urea to a free NR solution in methanol. As seen from Figure S20, the free NR also exhibit a decline of fluorescence intensity after urea treatment, with the extent of decrease similar to that of NR-loaded polymeric assemblies. Therefore, it can be concluded that urea does not have effect on the morphological change of multiblock copolymers, thus ruling out the role of hydrogen bonding in SDSA process.

Depolymerization-Induced Morphology Reversion (DPIMR)

In view of redox-responsive CDI linkages in our design, we further envisioned that whether the cleavage of multiblock polymers enables a potential depolymerization-induced morphology reversion (DPIMR). To validate this hypothesis, we treated the polymeric assemblies with 10 mM GSH. The properties of assemblies during GSH treatment were characterized by DLS, SLS and TEM. In brief, the sizes of polymeric assemblies after GSH treatment for different time were determined by a Zetasizer Nano ZS dynamic light-scattering (DLS) instrument (Malvern, UK) at 25 °C at an angle of 90°. Thereafter, the morphologies of P3 and P4 assemblies after GSH treatment were monitored by a combination of DLS/SLS analysis, and the obtained R_H, R_G and R_G/R_H

were listed in Table S3. In addition, P3 and P4 assemblies after GSH treatment were observed directly by TEM.

To further explore the potential of hypersensitive and efficient release of payloads in reducing environments, we studied the change of fluorescence intensity of NR-loaded assemblies incubated with 10 mM GSH for different times. The rate of fluorescence intensity decrease was calculated and normalized by eq S6:

$$\text{FL intensity decrease (\%)} = \frac{I_0 - I}{I_0} \times 100\% \quad \text{(S6)}$$

where I represents the intensity of NR loaded in multiblock copolymer assemblies at different time points, I_0 is the original fluorescence intensity before treatment.

Forster Resonance Energy Transfer (FRET) Measurement

DOX and Cy5 were co-loaded in multiblock copolymers assemblies by a film-forming method. In brief, 1 mL of DOX (1 mg mL^{-1}) and Cy5 (2 mg mL^{-1}) solutions in DCM was added in bottle, and dried by a flow dry argon. Then, 5 mL of polymer dispersions in water were added into the bottle and ultrasonated for 2 h. The solution was transferred to a dialysis bag (MWCO 3500) and dialyzed against water for 24 h, changing the water every 3 h. Finally, the solution was centrifugalized for 10 min at 3000 r min^{-1} and filtered through a 0.45 μm pore-sized syringe filter (Millipore, Carrigtwohill, Co. Cork, Ireland). For FRET measurements, the polymeric assemblies encapsulating DOX and Cy5 were treated with 10 mM of GSH and determined with an F-4600 FL spectrophotometer (Hitachi, Ltd., Japan) for different time points. The donor (DOX) was excited at 480 nm and the emission spectra were recorded at all

wavelengths simultaneously. The ratio of fluorescence intensity at 594 nm to that at 670 nm was normalized and plotted over time.

DOX Loading and Release

DOX as a model hydrophobic anticancer drug was loaded into MBC assemblies. In brief, hydrophilic DOX·HCl was dispersed in THF and desalted in the presence of excess amount of TEA under ultrasonic condition. The solution was added dropwise into MBC assemblies with stirring at a feed ratio of 30 wt%. Then the solution was transferred into a dialysis bag (MWCO 3500) and dialyzed against phosphate buffered solution (PBS, pH 7.4) for 3 d with changing PBS once 3 h. Finally, the solution was centrifugalized for 15 min at 3000 r min-1 and filtered through a 0.22 μm pore-sized syringe filter.

Drug loading content and encapsulation efficiency were calculated according to the following equations:

loading content (%) = weight of loaded drugs / weight of drug-loaded micelles × 100% (S7)

encapsulation efficiency (%) = weight of loaded drugs / weight of feeding drugs × 100% (S8)

The release of DOX was evaluated with a dialysis method in phosphate buffer solution (PBS, 10 mM, pH 7.4) with or without 10 mM GSH under shaking. At desired time intervals, 2 mL of release media was sampled and replenished with an equal volume of fresh media. The release experiments were conducted in triplicate. The

amount of DOX released was determined by a UV-Vis spectrometer (UV-2600, Shanghai Techcomp Instrument Co., Ltd, Shanghai, China).

Cell Internalization

The cellular uptake of DOX-loaded multiblock copolymers assemblies were conducted by flow cytometry and a confocal laser scanning microscope (CLSM). For CLSM, breast cancer (MCF-7) cells were seeded in a six-well plate (a coverslip was placed in every well before use) at a density of 1×10^5 cells per well and cultured overnight. To determine whether particle morphologies had effect on intracellular DOX delivery, the cells were pre-treated with buthionine sulphoximine (BSO) for 12 h. Then the MBC assemblies were added separately into the plate with a consistent drug concentration of 10 μg mL^{-1} and incubated for another 4 h. Next, the medium was removed and the plate was washed with PBS for three times. Then the cells were fixed with 4% formaldehyde for 30 min and stained with DAPI for 10 min. At last, the coverslips were mounted with 50% glycerol solution and observed on a CLSM (Olympus FV1000, Japan). For flow cytometry, DOX-loaded multiblock copolymers assemblies were added separately into a six-well plate with 5×10^5 cells per well at a consistent drug concentration of 10 μg mL^{-1}, and incubated for 4 h. After removing the medium, the plate was washed with PBS for three times. Then the cells were digested by trypsin, centrifuged, and re-suspended in 0.5 mL PBS for flow cytometer measurement (Beckman Cytoflex, USA).

MTT Assay

MTT assay was performed to evaluate the cytotoxicity of empty MBC assemblies and DOX-loaded formulations. Briefly, fibroblasts cells (L929) or MCF-7 were seeded in 96-well plates at a density of 5× 10^3 cells per well and cultured overnight. Then the drug-free and DOX-loaded formulations with different concentrations were added into the plates and incubated for 48 h. Afterward, 20 μL of MTT solution (5mg mL^{-1}) was added into each well for another 2 h of incubation. Finally, the solution in each well was replaced by 200 μL of DMSO. After shaking the plates for 10 min to dissolve the formazan crystals, the absorption intensity at 490 nm was recorded on a microplate reader (DNM-9602, Nanjing Perlove Medical Equipment Co., Ltd., China).

Computational Simulation

The interesting segment-driven self-assembly (SDSA) was visually verified by computational simulation using a dissipative particle dynamics (DPD) method. DPD simulation is a particle-based mesoscopic simulation technique originally introduced by Hoogerbrugge and Koelman in 1992,[S18] and further modified by Español and Warren.[S19] It has been established as a powerful tool to investigate the self-assembly of amphiphilic copolymers.[S20] In this method, a series of soft interacting particles named beads are considered interacting with each other and each particle represents a small volume of fluid containing many atoms. The force between each pair of beads is composed of three different pairwise additive parts:

$$\boldsymbol{f}_i = \sum_{j \neq i} (\boldsymbol{F}_{ij}^C + \boldsymbol{F}_{ij}^D + \boldsymbol{F}_{ij}^R) \quad \text{(S9)}$$

where $\boldsymbol{F}_{ij}^C$, $\boldsymbol{F}_{ij}^D$ and $\boldsymbol{F}_{ij}^R$ represent conservative, dissipative, and random forces, respectively, and the total force is pairwise additive force and runs over all particles

within a certain cutoff radius r_c. As this is the only length-scale in the system, cutoff radius is always used as the unit of length, $r_c = 1$. The conservative force $\boldsymbol{F}_{ij}^{C}$ is a soft repulsive potential between different nonbonded beads,

$$\boldsymbol{F}_{ij}^{C} = \begin{cases} \alpha_{ij}(1 - r_{ij})\,\hat{\boldsymbol{r}}_{ij}, & r_{ij} < 1 \\ 0, & r_{ij} > 1 \end{cases} \tag{S10}$$

where α_{ij} is the repulsive interaction parameter between particles i and j, and r_{ij} is the magnitude of the bead-bead vector. $\hat{\boldsymbol{r}}_{ij}$ is the unit vector joining beads i and j.

The dissipative force is a friction force that reduces the velocity differences between DPD beads, which is given by

$$\boldsymbol{F}_{ij}^{D} = -\gamma\omega^{D}(r_{ij})(\hat{\boldsymbol{r}}_{ij} \cdot \boldsymbol{v}_{ij})\hat{\boldsymbol{r}}_{ij} \ , \tag{S11}$$

where γ is the friction coefficient controlling the magnitude of dissipative force, $\boldsymbol{v}_{ij} = \boldsymbol{v}_i - \boldsymbol{v}_j$ and ω^D is a γ-dependent weight function providing the range of interaction for DPD particles.

The random force compensates the loss of energy due to the dissipative force reducing the relative momentum. The random force acts between all pairs of particles as

$$\boldsymbol{F}_{ij}^{R} = \sigma\omega^{R}(r_{ij})\theta_{ij}\hat{\boldsymbol{r}}_{ij} \ , \tag{S12}$$

where σ is the noise parameter that affects the intensity of the random force. ω^R is also a γ-dependent weight function and θ_{ij} is a randomly fluctuating variable with Gaussian statistics. The friction coefficient γ and noise magnitude σ are related by the fluctuation-dissipation theorem in the following equation:

$$\sigma^2 = 2\gamma k_B T \ , \tag{S13}$$

where k_B is the Boltzmann constant and T is the equilibrium temperature of the system. In the simulation, the units of mass, length, time, and energy are scaled by particle mass m, cutoff distance r_c, time τ, and thermal energy k_BT, respectively.

The facility of DPD simulation is that we need only to obtain the repulsion parameters for different beads. Groot and Warren have proposed the relationship between α_{ij} and the Flory-Huggins parameters (χ_{ij}) to determine the conservative force:[S21]

$$F_{ij} = \begin{cases} a_{ii} + 3.27\chi_{ij} & \rho = 3 \\ a_{ii} + 1.45\chi_{ij} & \rho = 5 \end{cases} \quad \text{(S14)}$$

where ρ is the density, a_{ii} is the repulsion parameter between particles of the same type. The bead density of the system is close to that of water with ρ = 3, cutoff radius is always used as the unit of length, $r_c = k_BT = 1$. Thus, a_{ij} can be estimated from

$$a_{ij} \approx 25 + 3.27\chi_{ij}\,, \quad \text{(S15)}$$

where a_{ii} = 25 leads to the compressibility of water. If species i and j are fairly compatible, $\chi_{ij} \approx 0$ and $\alpha_{ij} \approx 25$. As incompatibility between i and j increases, α_{ij} increases from 25.[S22, S23] In our study, we consider an aqueous solution (W) of multiblock copolymers. The multiblock copolymers are molded as $(L_mCE_nC)_xL_mCE_n$, where L, E and C represent hydrophobic PCL blocks, hydrophilic PEG segments, and cystine-derivative linkers, respectively. The segment chain lengths and block numbers could be controlled by varying the m, n and x values. The interaction parameters are chosen in an attempt to retain the characteristic interactions associated with W, L, E and C beads. According to previous reports, the repulsive parameter between two alike particles is set to α_{ij} = 25.0 (α_{WW}, α_{LL}, α_{EE}, α_{CC}, α_{LC}) to reflect the correct compressibility

of these DPD beads at room temperature in dilute solution.[S24-S26] Moreover, the interaction parameters between the hydrophobic and hydrophilic segments were set as $\alpha_{LE} = \alpha_{CE} = 50$, suggesting that the hydrophobic and hydrophilic components are incompatible and phase-segregated in water.[S24, S25, S27-S29] To model the amphiphilic nature of multiblock copolymers, the interaction parameter between solvophobic segments and solvent were set as $\alpha_{LW} = \alpha_{CW} = 80$.[S27-S30] It is worth noting that the χ-parameter between PEG and water was taken as 0.30 proposed by Groot and Rabone,[S31] which was fitted from experimental adsorption data by Seaki et al.[S32] Hence, the interaction parameter between PEG and water was calculated to be $\alpha_{EW} = 25.98$ according to equation S13.

We carried out the simulation in a cubic simulation box of size $20 \times 20 \times 20r_c^3$ with a periodic boundary condition to eliminate the finite size effects. The total beads were 24,000, the spring constant C was chosen as 10.0 and the time step was taken as 0.05. The simulation steps of 100,000 were adopted, which are sufficient for achieving simulation equilibrium and steady results (Fig.S32). All the computational works were performed using DPD program incorporated in the software Materials Studio 5.0 software (Accelrys) installed on a DELL PowerEdge SC430 server.

Statistical Analysis

The quantitative data obtained were expressed as means ± standard deviations (SD). Statistical analysis was carried out using the Statistical Package for the Social Sciences (IBM SPSS Statistics software, Version 19, IBM, New York, USA). Student's t-test or

one-way analysis of variance (ANOVA) was performed to determine the statistical significance within the data at 95% confidence levels ($P < 0.05$).

Supporting Figures and Tables

Scheme S1. Synthesis of CDI.

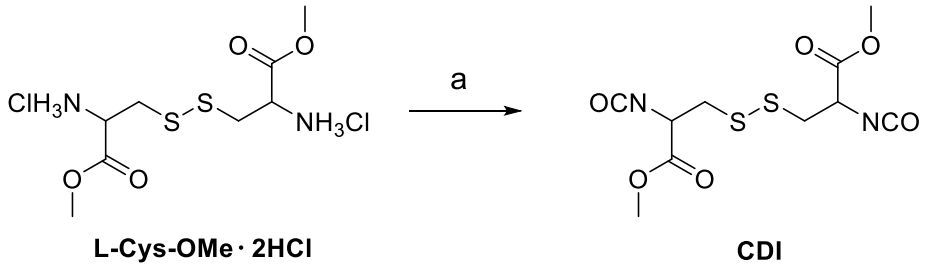

Reagents and conditions: (a) triphosgene, CH_2Cl_2, pyridine, -5 °C, 5 h (75% yield).

Scheme S2. Synthesis of multiblock copolymers with different block numbers (P2-P4).

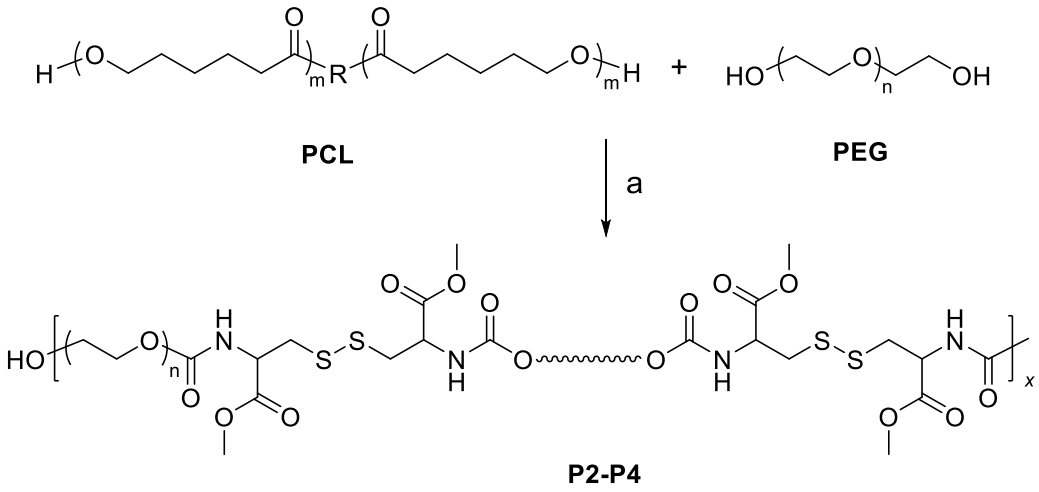

Reagents and conditions: (a) CDI (Scheme S1), stannous octanoate, DCE, 60 °C, 24 h, 80 °C, 24 h (83% yield).

Scheme S3. Synthesis of multiblock copolymers with different block sequence (P4-D)

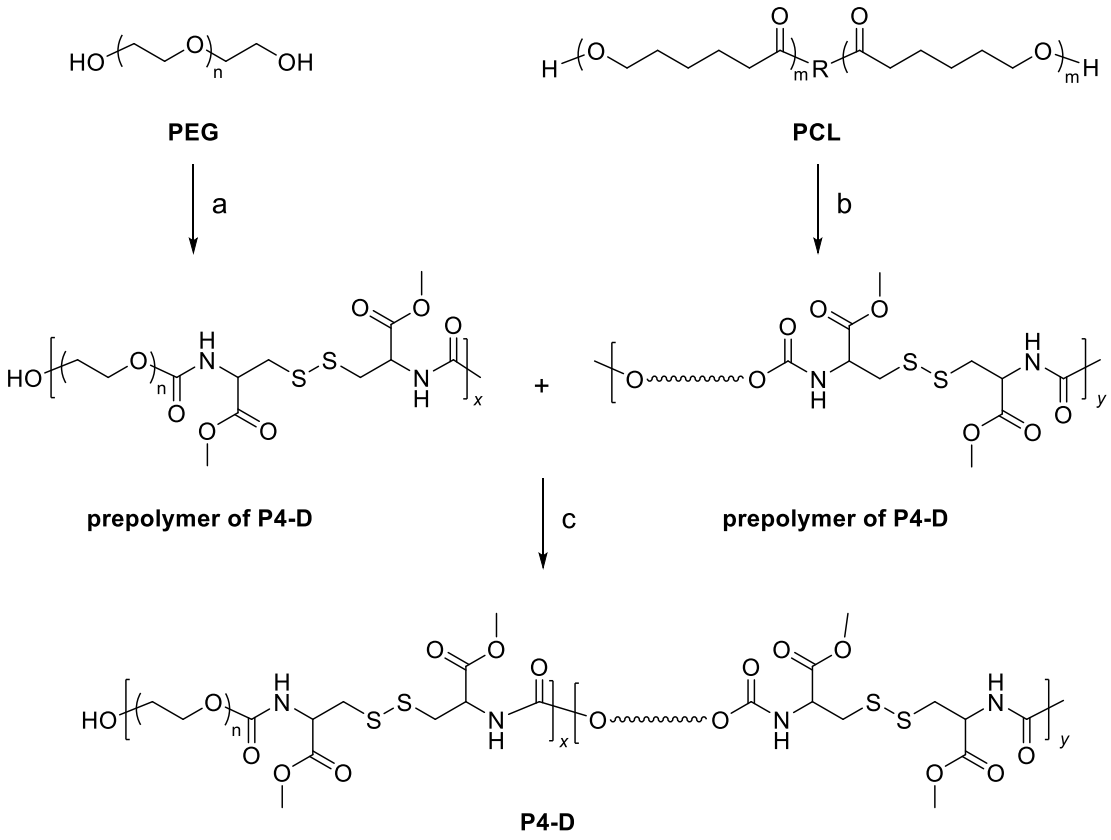

Reagents and conditions: (a) CDI, stannous octanoate, DCE, 70°C, 24 h. (b) CDI, stannous octanoate, DCE, 70 °C, 24h. (c) CDI, stannous octanoate, DCE, 80 °C, 24 h (78% yield).

Scheme S4. Synthesis of multiblock copolymers with different linkers (P4-L).

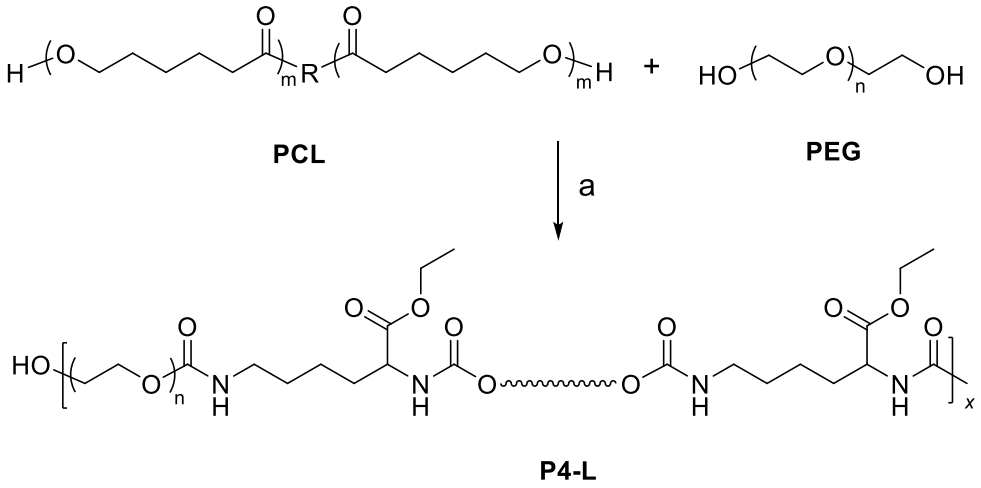

Reagents and conditions: (a) LDI, stannous octanoate, DCE, 80 °C, 24 h (82% yield).

Scheme S5. Synthesis of diblock copolymer P1

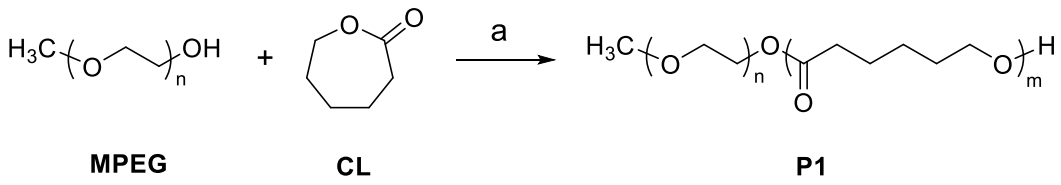

Reagents and conditions: (a) stannous octanoate, DCE, 115°C, 24 h (80% yield).

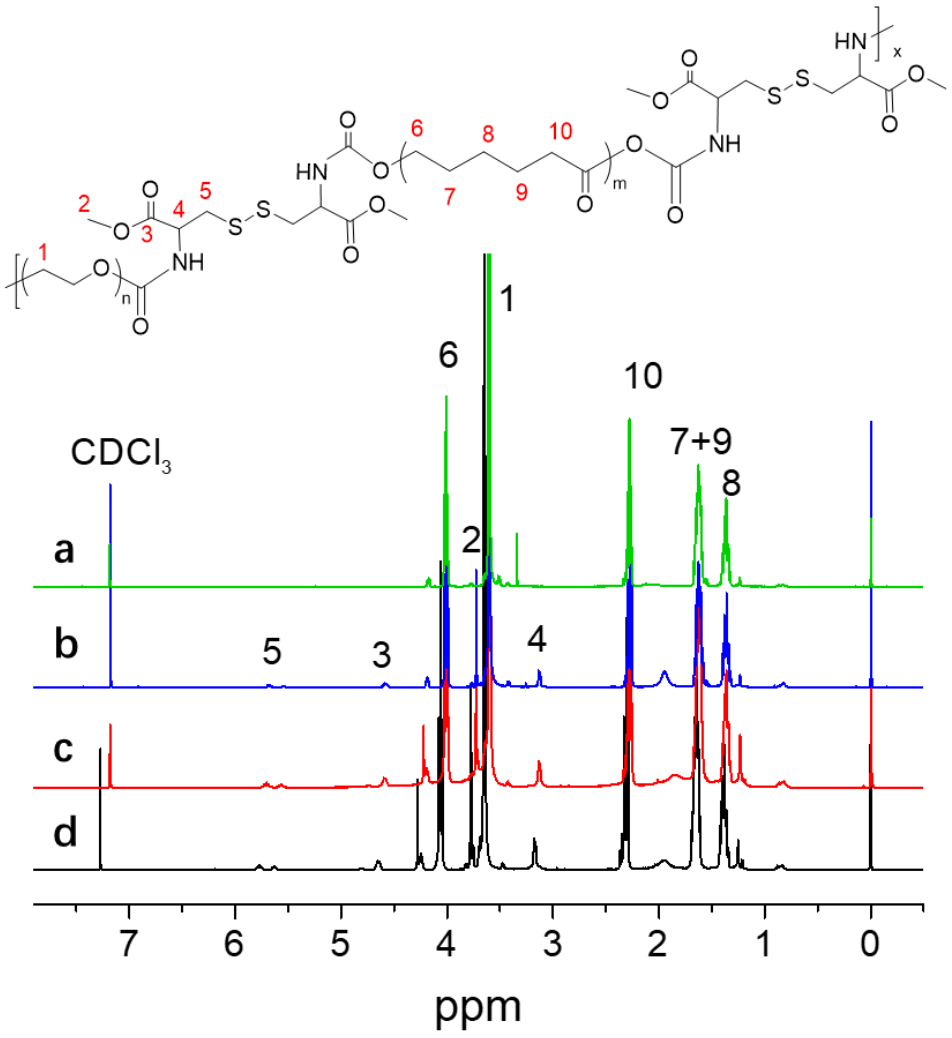

Figure S1. 400 MHz ^{1}H NMR spectra of multiblock copolymers in $CDCl_3$: (a) P1, (b) P2, (c) P3 and (d) P4.

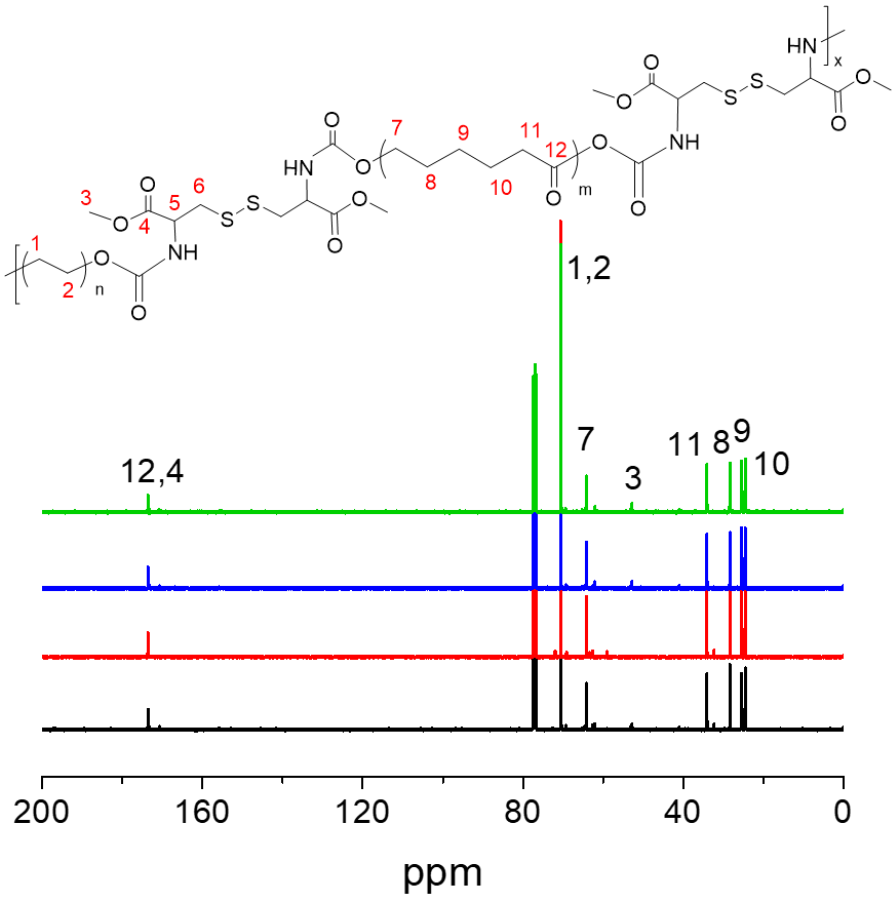

Figure S2. 400 MHz ^{13}C NMR spectra of multiblock copolymers in $CDCl_3$: (a) P1, (b) P2, (c) P3 and (d) P4.

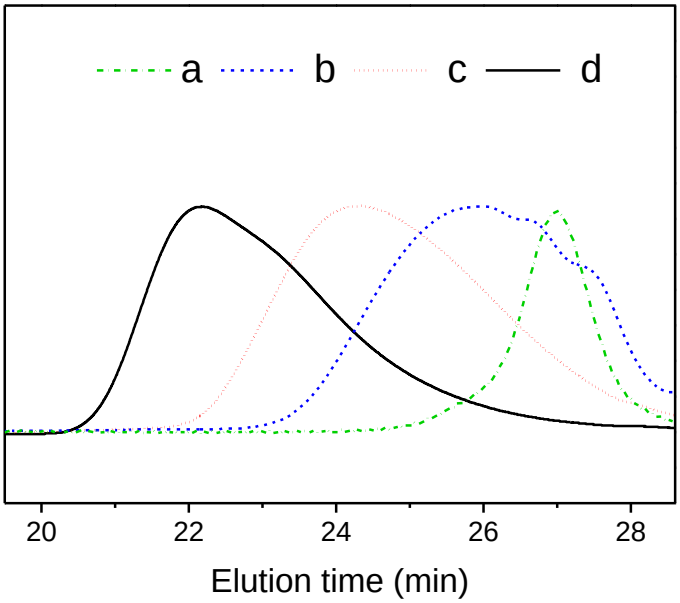

Figure S3. GPC spectra of multiblock copolymers in $CDCl_3$: (a) P1, (b) P2, (c) P3 and (d) P4.

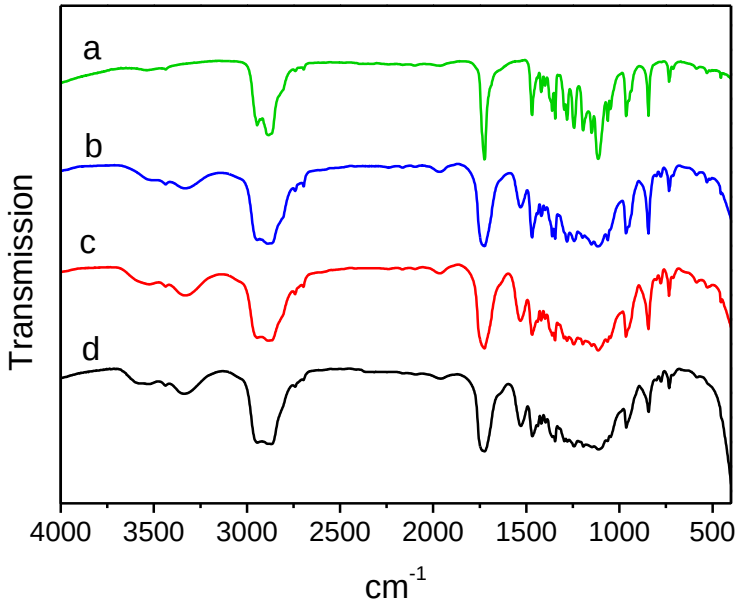

Figure S4. FTIR spectra of multiblock copolymers: (a) P1, (b) P2, (c) P3 and (d) P4.

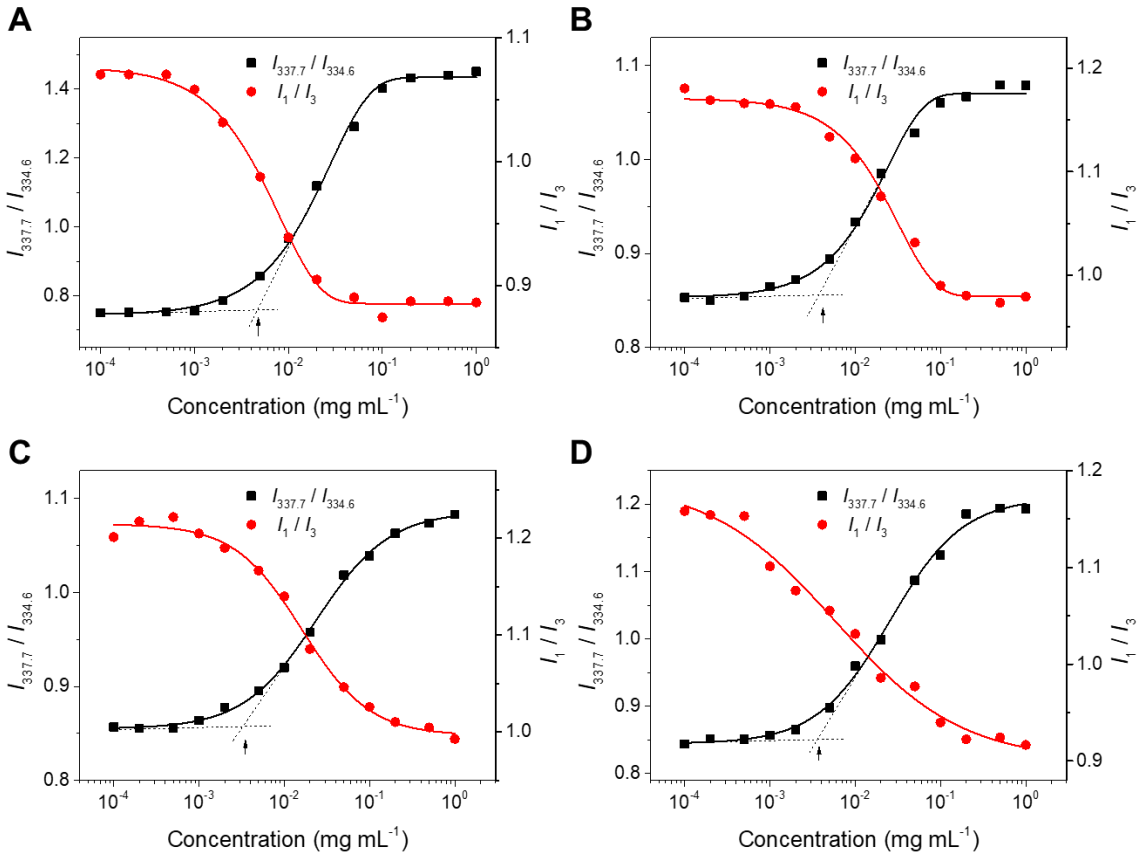

Figure S5. (A) Plots of the fluorescence intensity ratios $I_{337.7}/I_{334.6}$ (from pyrene excitation spectra) and I_1/I_3 (from pyrene pyrene emission spectra) as a function of the concentrations (log C) of (A) P1, (B) P2, (C) P3 and (D) P4 assemblies. The CAC values were obtained from the intersection of the two trend lines shown by the arrows, which were estimated to be 2.6×10^{-3}, 2.5×10^{-3}, 2.7×10^{-3}, 3.7×10^{-3} mg mL^{-1}, respectively, for P1, P2, P3 and P4.

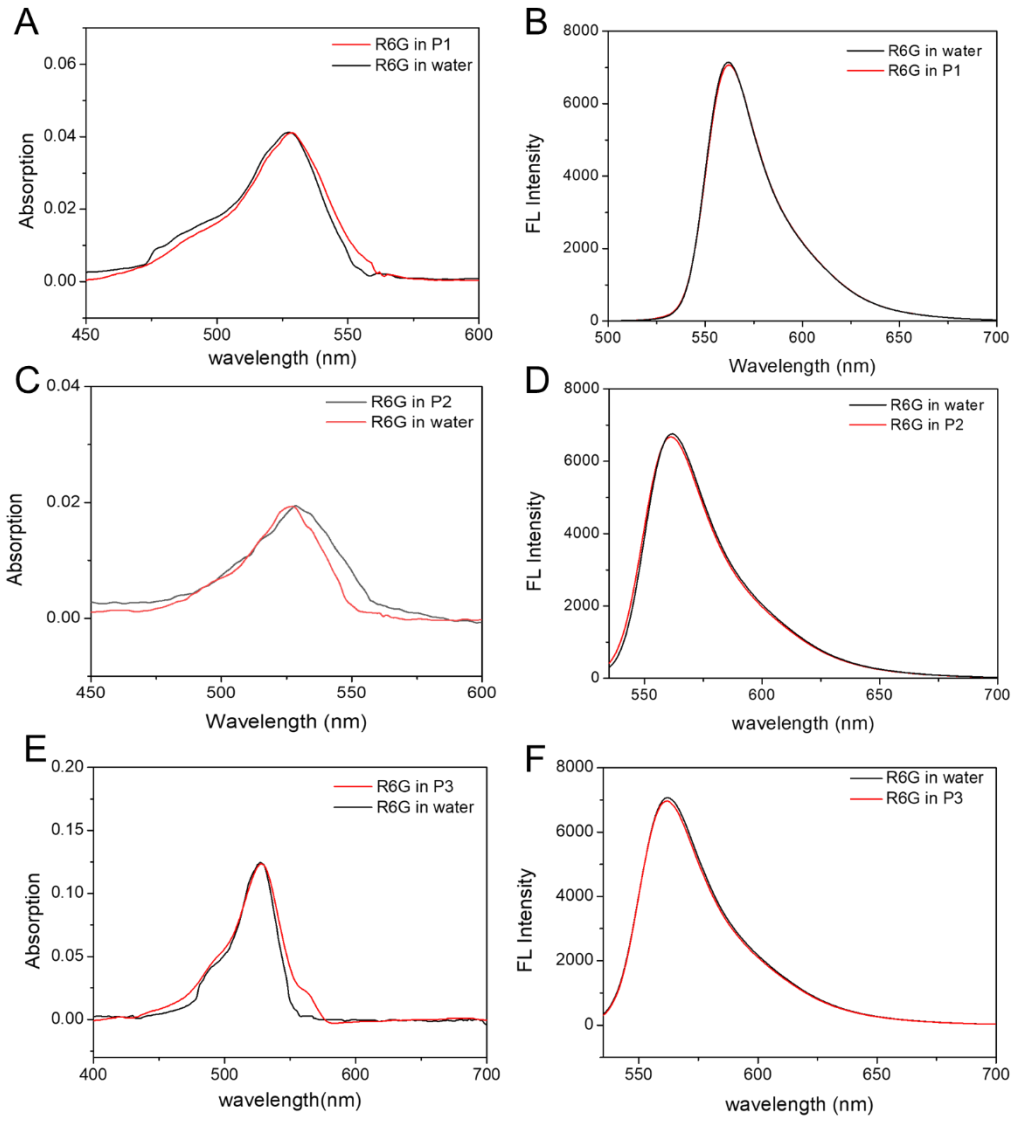

Figure S6. UV-vis spectra (A, C, E) and fluorescence emission spectra (B, D, F) (λ_{ex} = 526 nm) of R6G in water or in the presence of P1 (A, B), P2 (C, D) and P3 (E, F) assemblies.

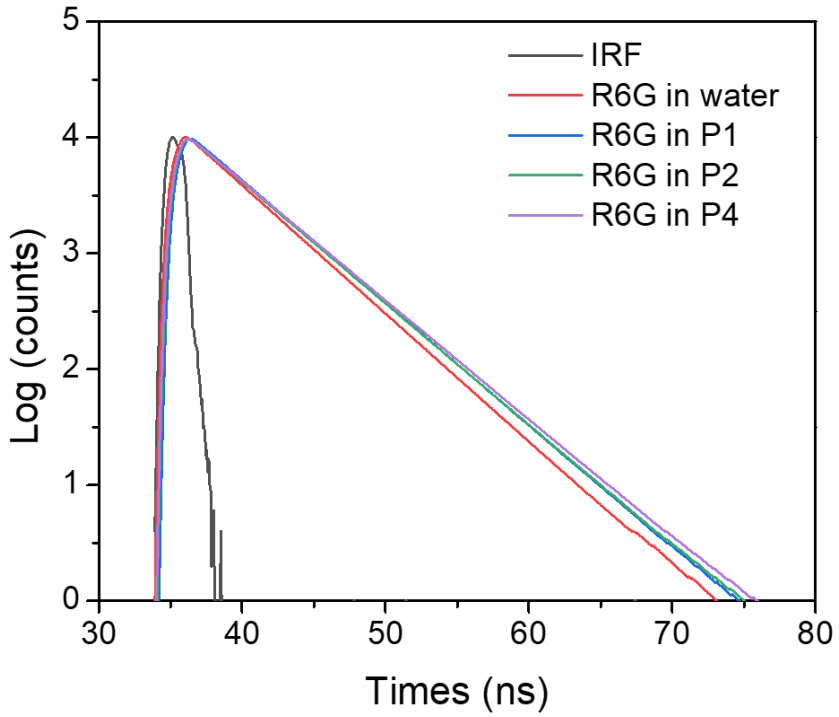

Figure S7. Fluorescence decay profiles for R6G dissolved in water and that encapsulated in multiblock copolymers assemblies. The instrument response function (IRF) was also included. The concentration of free R6G solution in water was adjusted so that the absorption intensity matches the intensity of R6G in assembled solutions. The lifetime values of R6G in water and that loaded in multiblock copolymers assemblies were listed in Table S2.

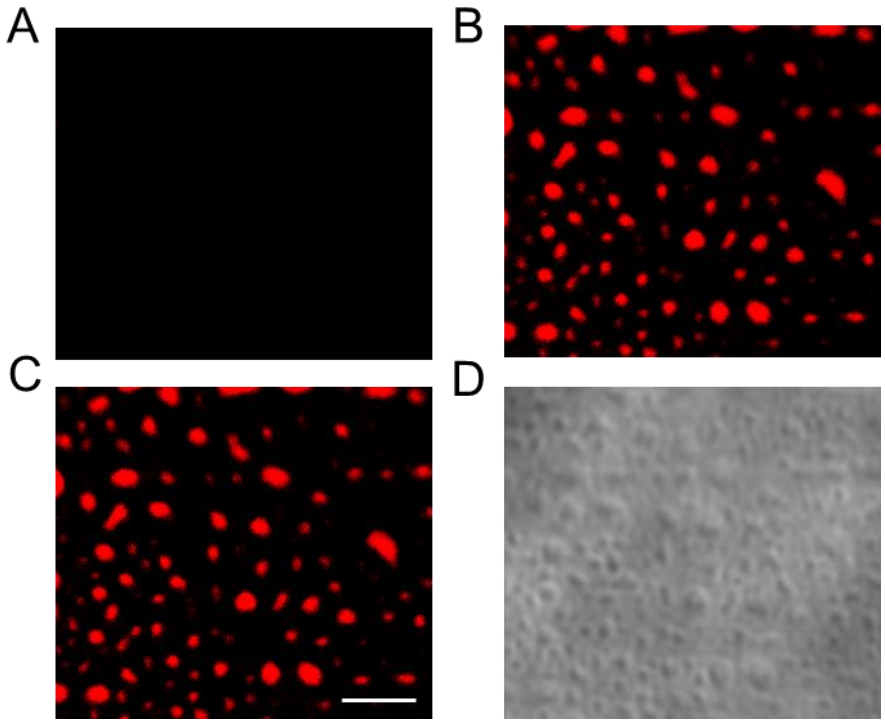

Figure S8. CLSM images of P1 assemblies loaded with R6G (hydrophilic) and NR (hydrophobic). (A) R6G (green), (B) NR (red), and (C) overlay of panels A and B. (D) Bright field images. The scale bar is 2 μm.

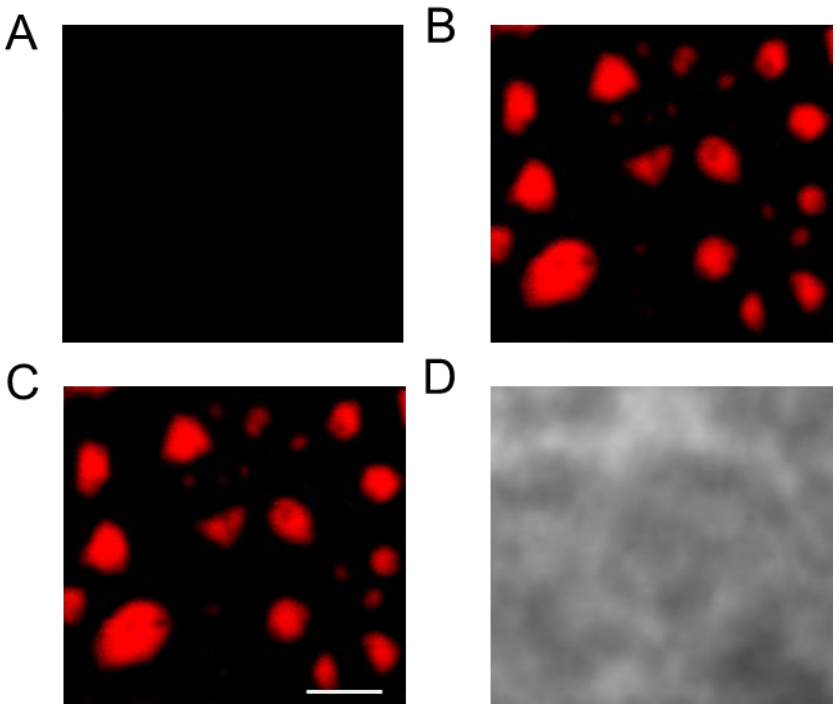

Figure S9. CLSM images of P2 assemblies loaded with R6G (hydrophilic) and NR (hydrophobic). (A) R6G (green), (B) NR (red), and (C) overlay of panels A and B. (D) Bright field images. The scale bar is 2 μm.

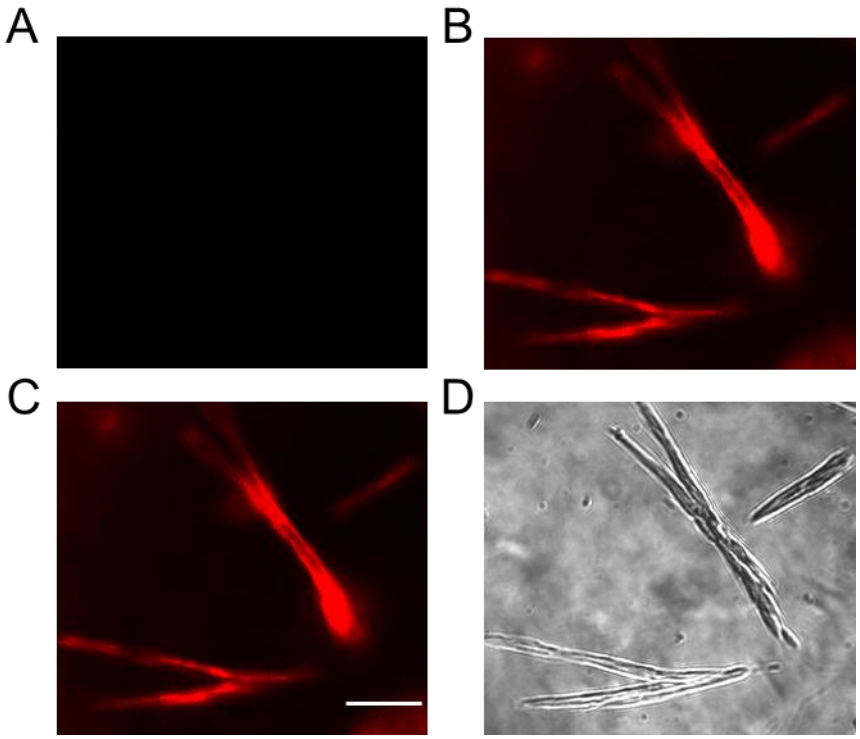

Figure S10. CLSM images of P3 assemblies loaded with R6G (hydrophilic) and NR (hydrophobic). (A) R6G (green), (B) NR (red), and (C) overlay of panels A and B. (D) Bright field images. The scale bar is 2 μm.

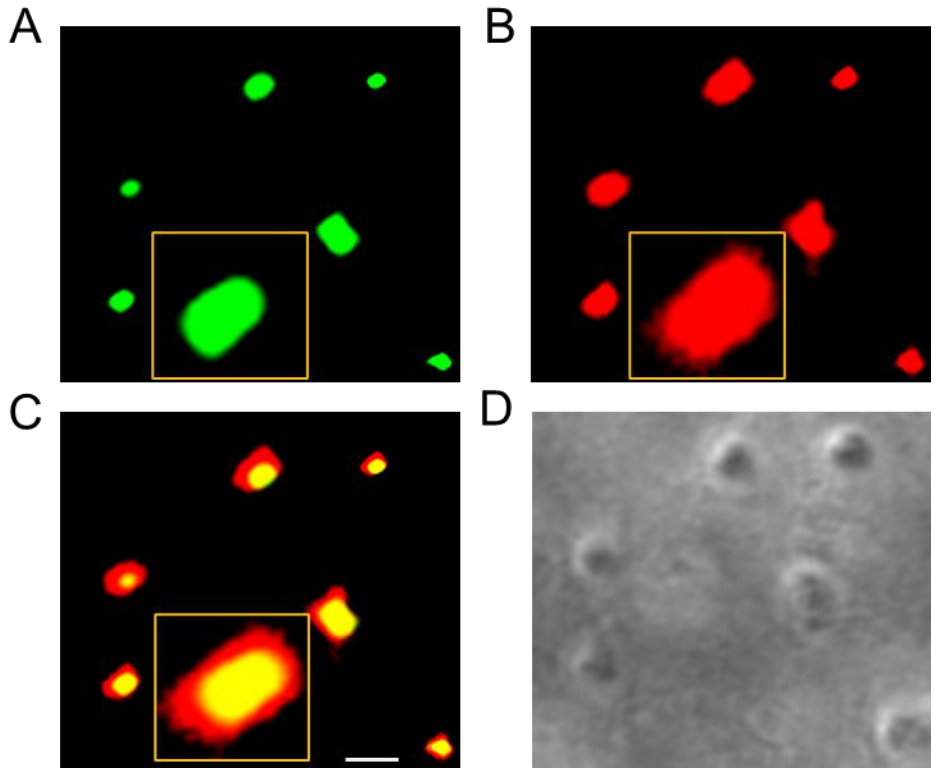

Figure S11. CLSM images of P4 assemblies loaded with R6G (hydrophilic) and NR (hydrophobic). (A) R6G (green), (B) NR (red), and (C) overlay of panels A and B. (D) Bright field images. The scale bar is 2 μm. Insets show a giant vesicular aggregate encapsulating R6G and NR.

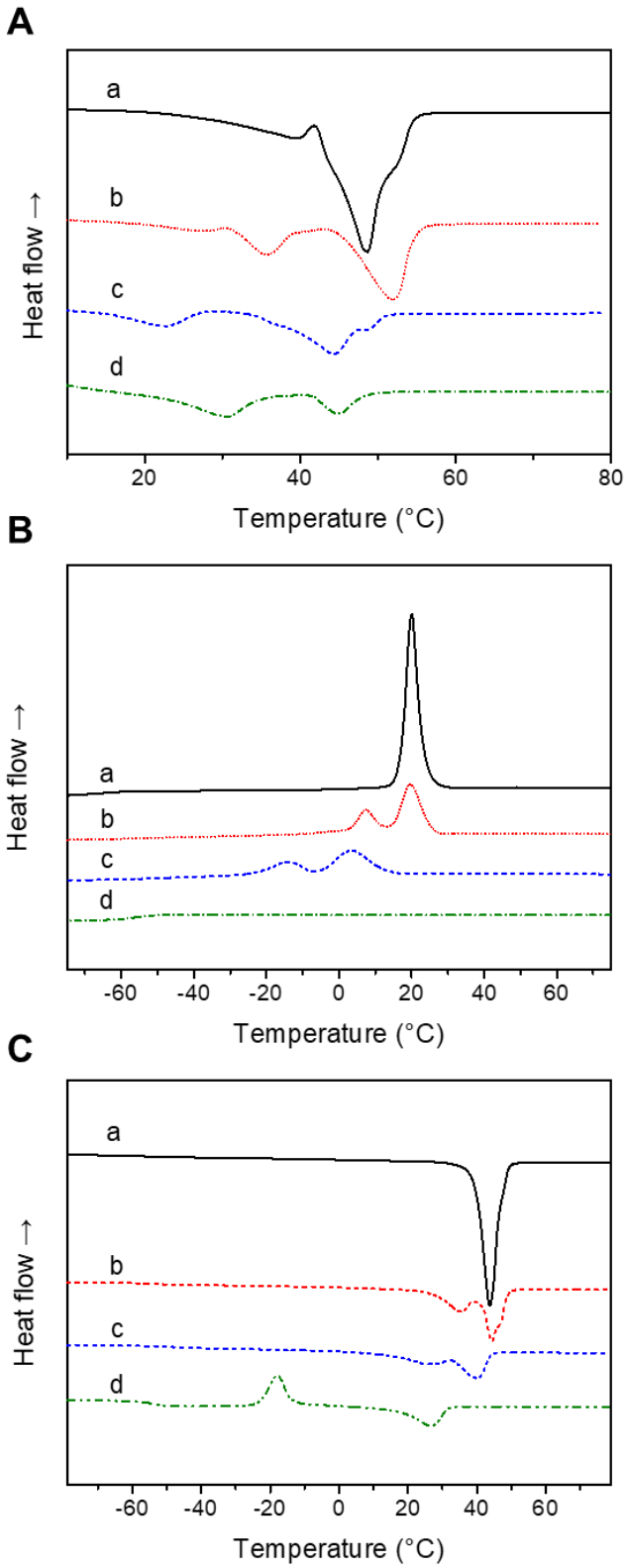

Figure S12. DSC thermograms of (a) P1, (b) P2, (c) P3 and (d) P4. A, B and D represent curves for first heating from 0 to 100 °C, first cooling from 100 to -80 °C and second heating from -80 to 100 °C, respectively.

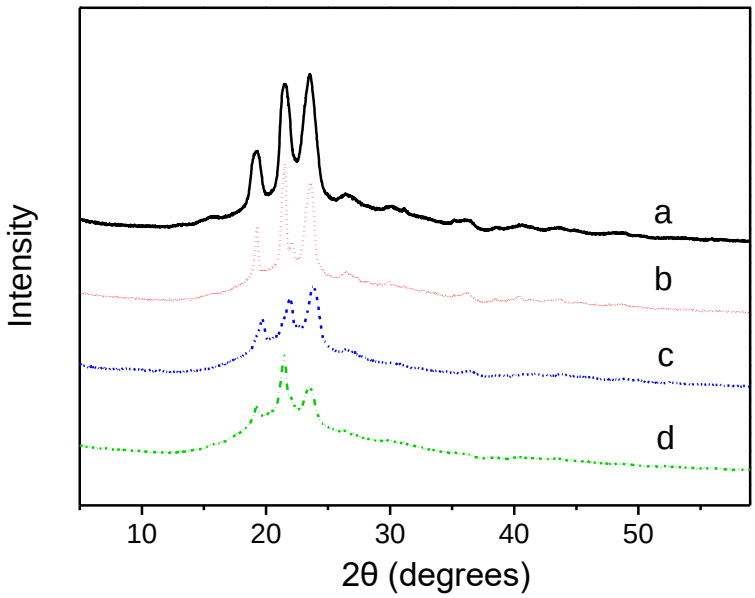

Figure S13. XRD curves of (a) P1, (b) P2, (c) P3 and (d) P4.

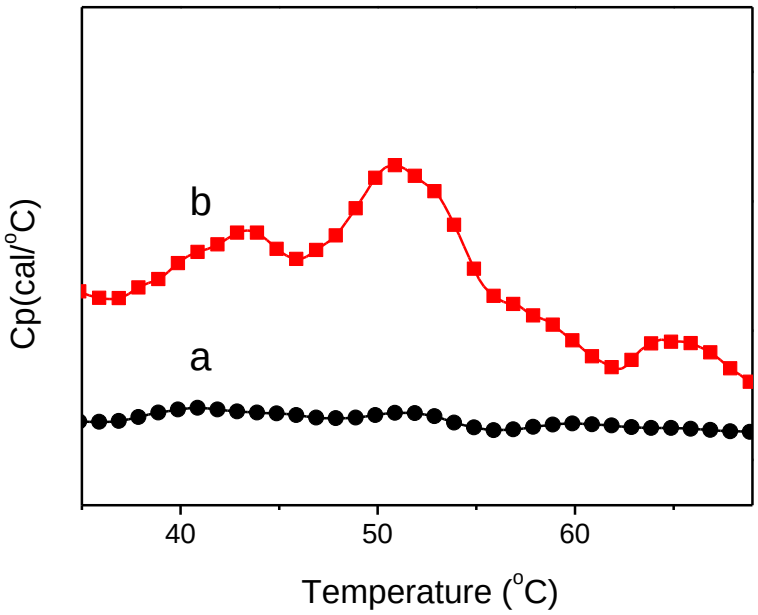

Figure S14. Super-sensitive DSC curves of (a) P2 and (b) P4 dispersions in an aqueous solution (1 mg mL^{-1}) at a heating rate of 1.5 °C min^{-1} from 20 to 80 °C.

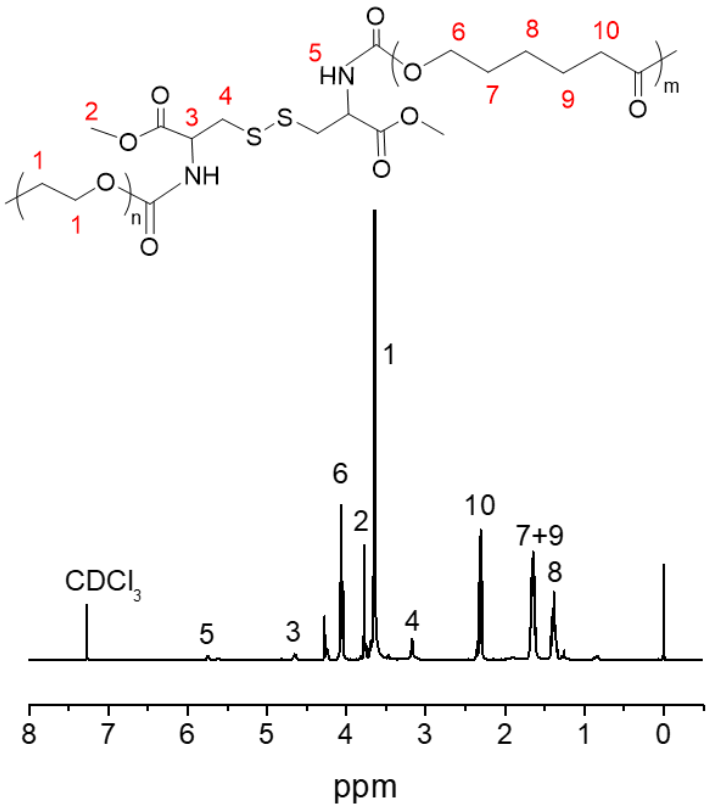

Figure S15. 400 MHz ^{1}H-NMR spectra of P4-D in $CDCl_3$.

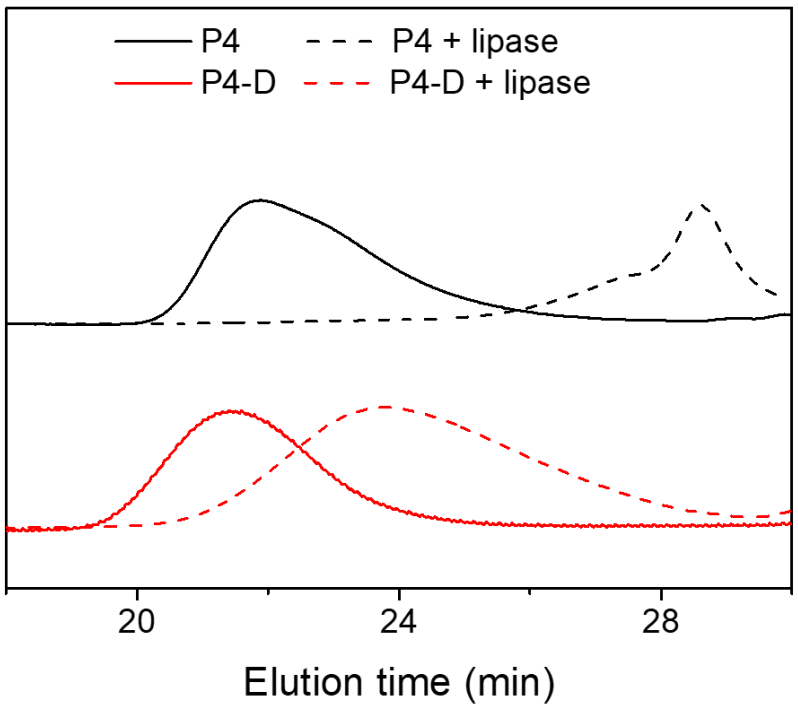

Figure S16. GPC spectra of P4 and P4-D after treatment with 0.2 mg mL^{-1} of lipase PS for 96 h.

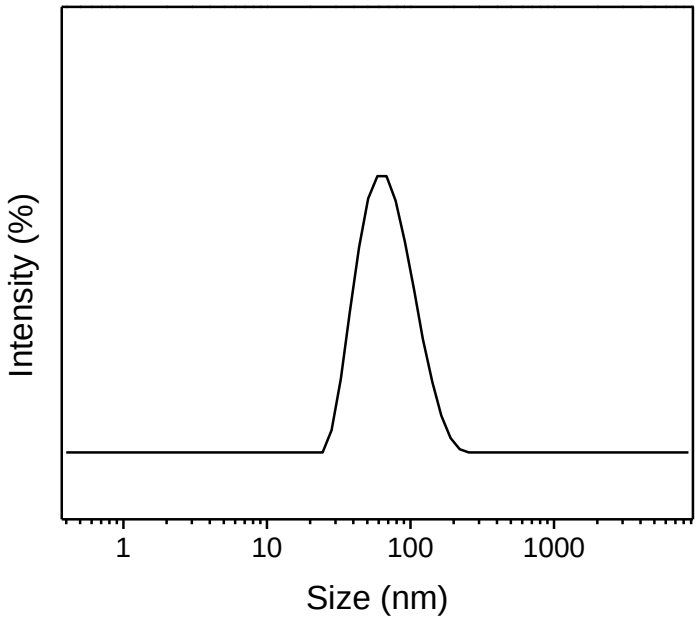

Figure S17. Size distribution profile of P4-D assemblies measured using a Zetasizer Nano ZS dynamic light-scattering (DLS) instrument (Malvern, UK) at 25 °C at an angle of 90°.

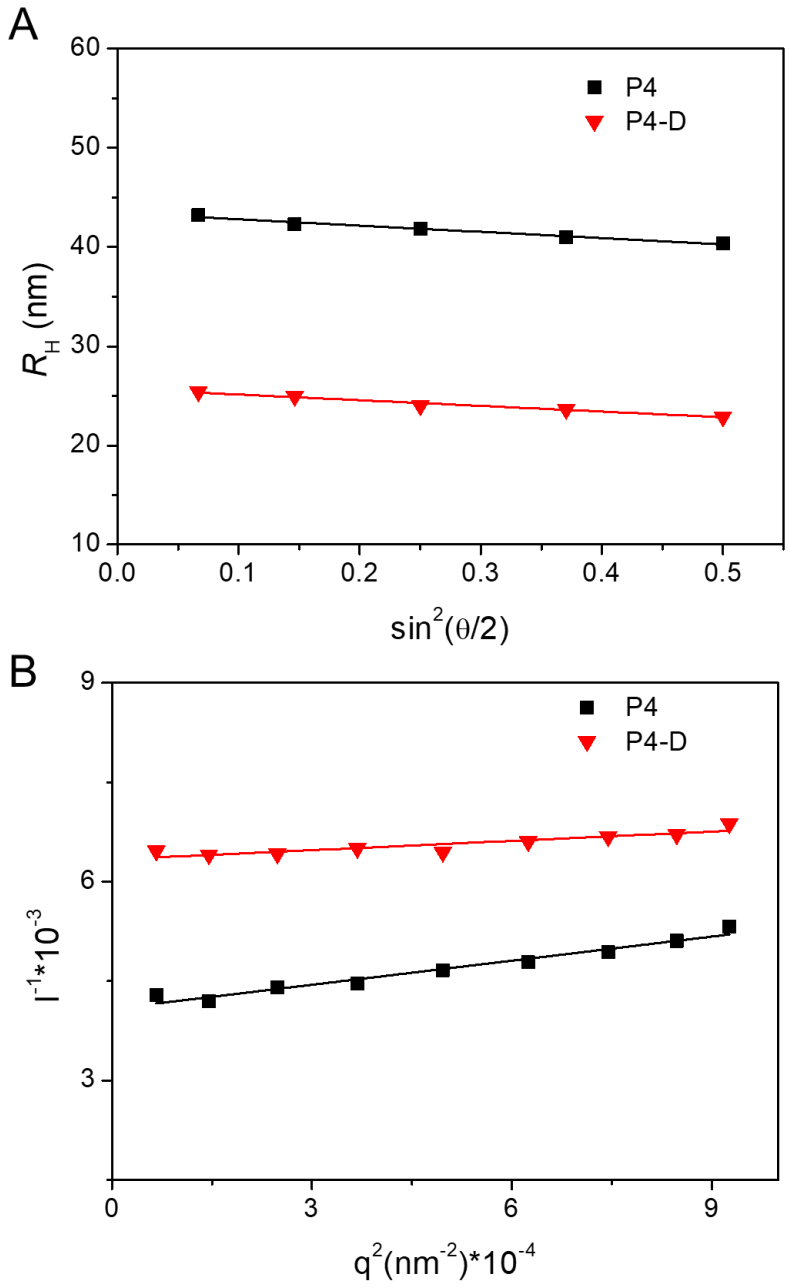

Figure S18. (A) Hydrodynamic radius associated functions at different incident angles determined by DLS. The R_H values of P4 and P4-D assemblies were determined to be 121 and 25.7 nm, respectively. (B) Typical Berry plots of P4 and P4-D assemblies measured at 25 °C using multi-angle SLS. The R_G values of P4 and P4-D assemblies were measured to be 120 and 20 nm, respectively. Accordingly, the R_G/R_H values of P4 and P4-D assemblies are 0.78 and 0.98 nm, respectively.

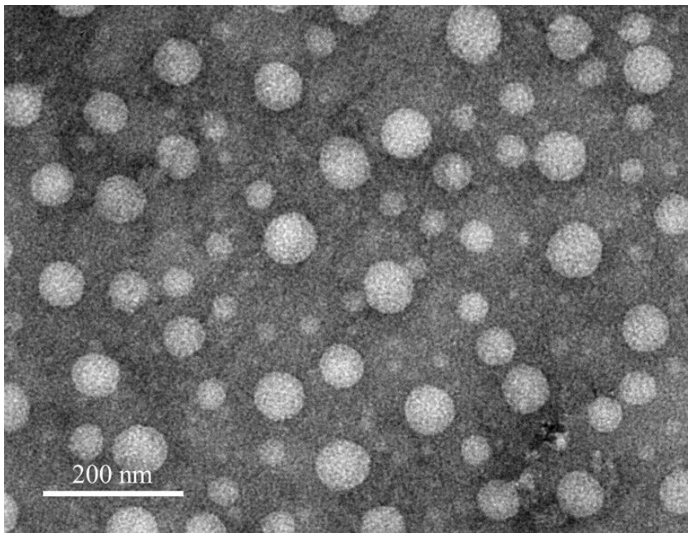

Figure S19. TEM images of P4-D self-assemblies. The bar is 200 nm.

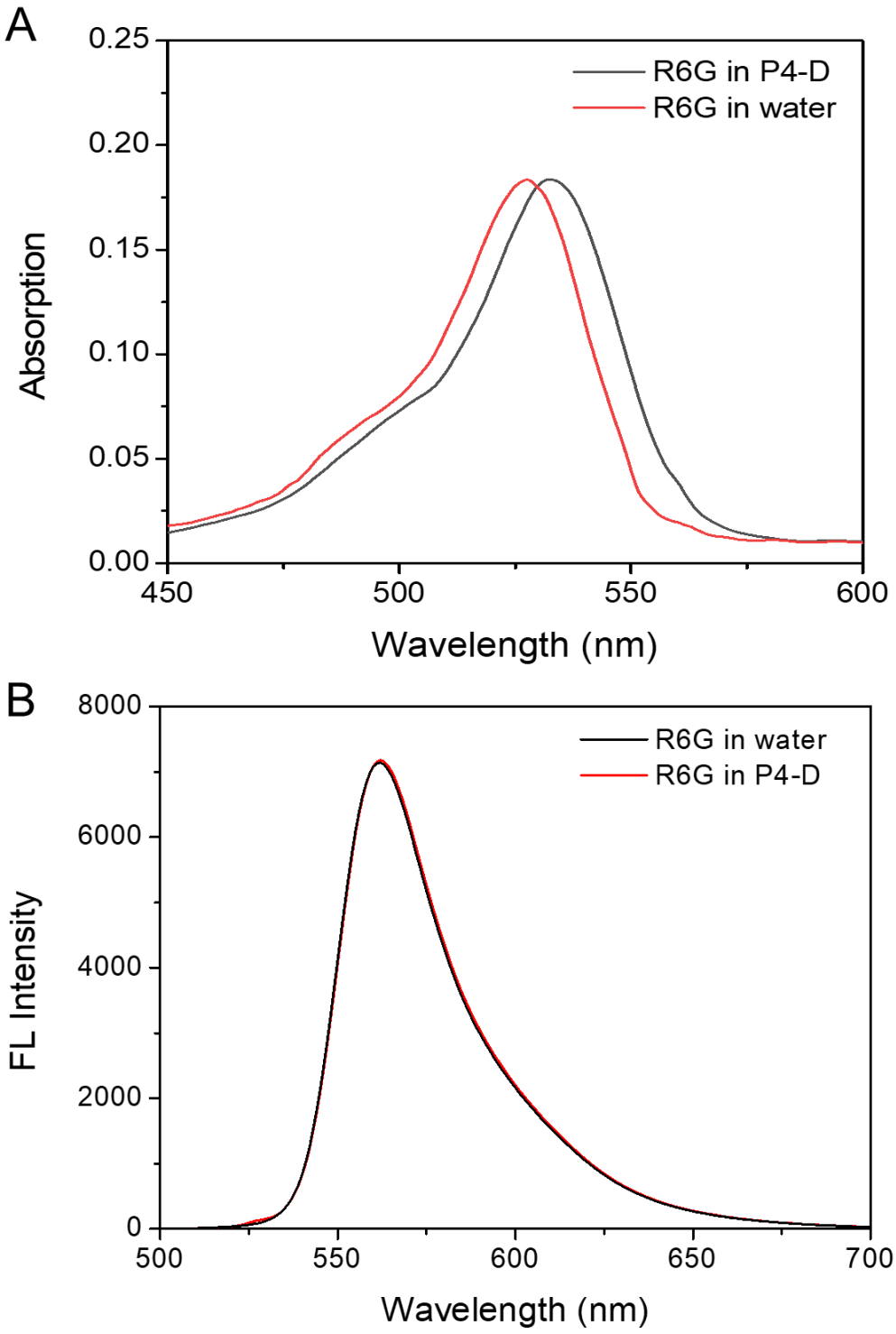

Figure S20. UV-vis spectra (A) and fluorescence emission spectra (λ_{ex} = 526 nm) (B) of R6G in water or P4-D assemblies.

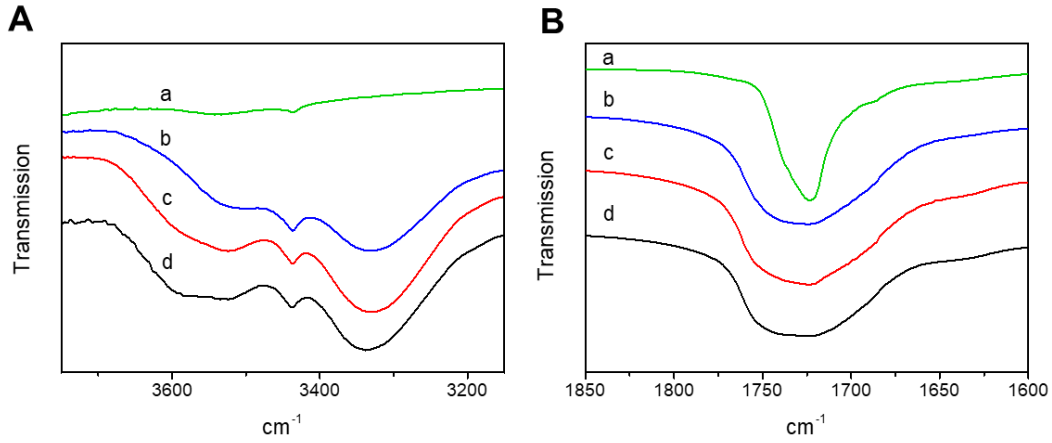

Figure S21. N-H stretching vibration region (A) and C=O stretching vibration region (B) in the FTIR spectra of multiblock copolymer films cast on KBr plates: (a) P1, (b) P2, (c) P3 and (d) P4.

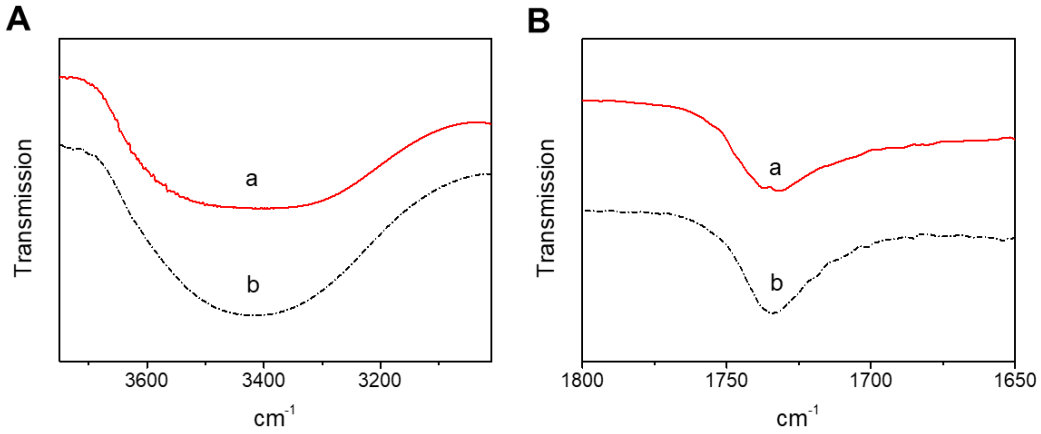

Figure S22. N-H stretching vibration region (A) and C=O stretching vibration region (B) in the FTIR spectra of multiblock copolymer dispersions in D_2O: (a) P2, and (b) P4.

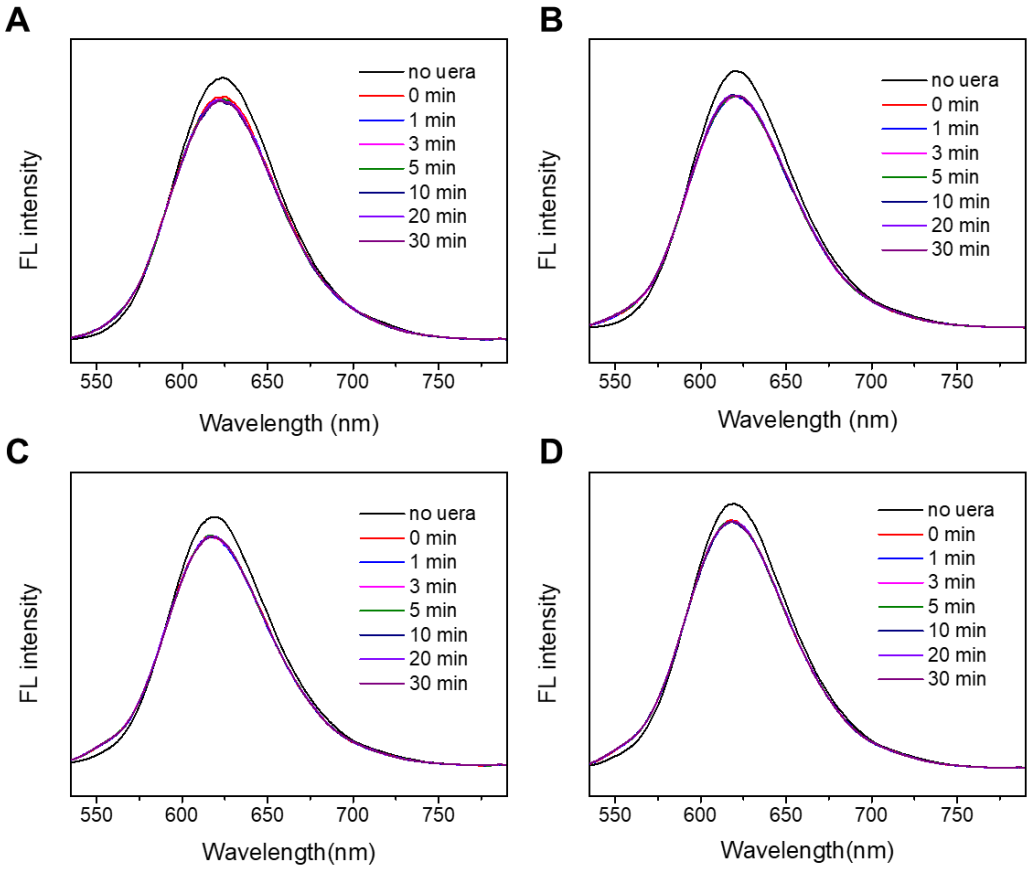

Figure S23. Fluorescence spectra of NR-loaded multiblock copolymer assemblies before and after addition of urea (7 M) for different times: (A) P1, (B) P2, (C) P3 and (D) P4.

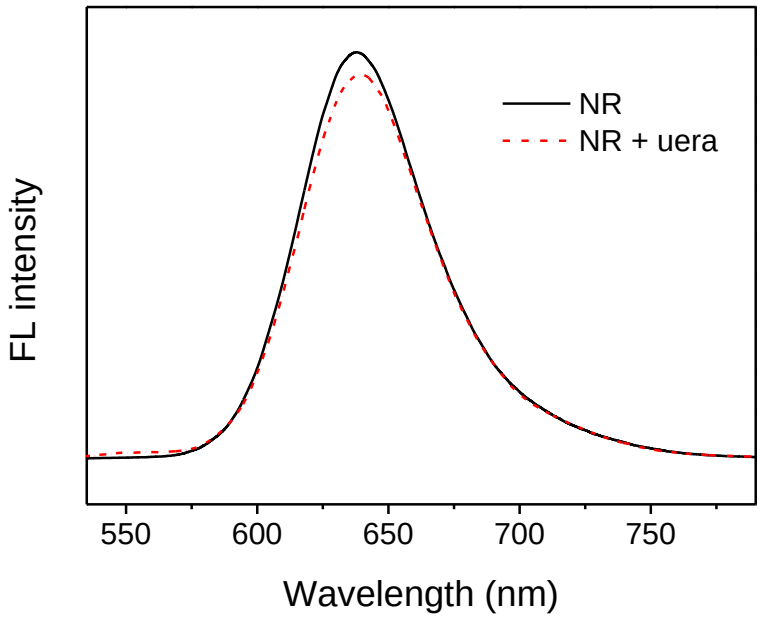

Figure S24. Fluorescence spectra of NR dissolved in methanol before and after addition of urea (7 M).

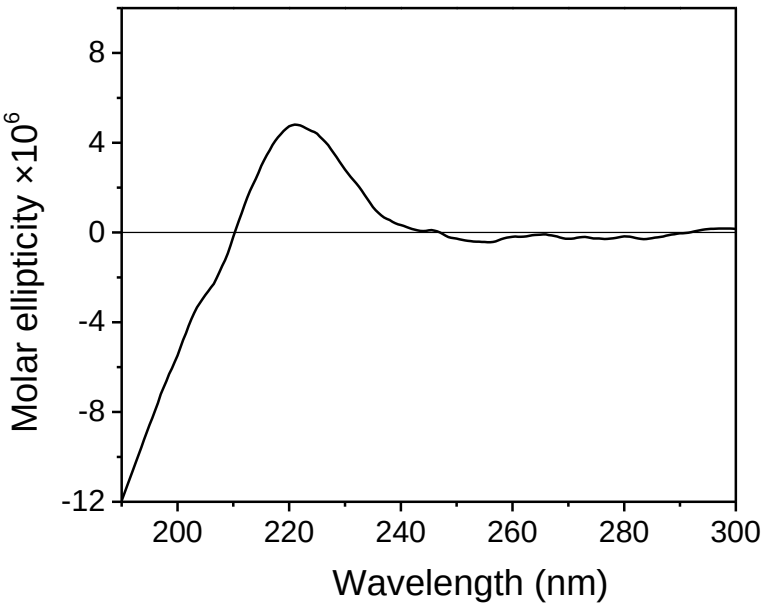

Figure S25. CD spectra of P4 assemblies

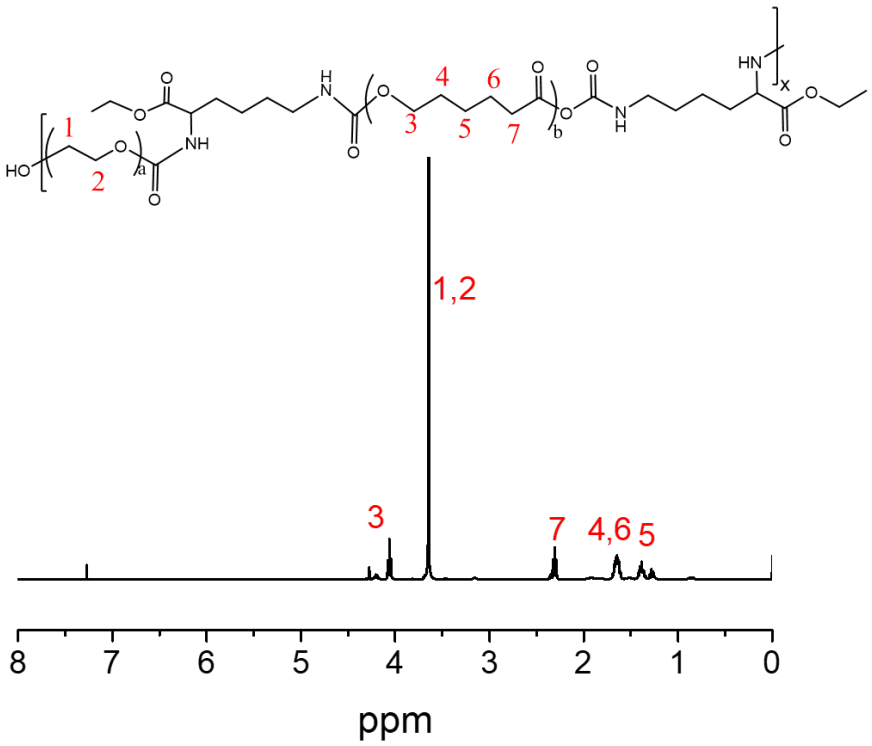

Figure S26. 400 MHz ^{1}H NMR spectra of P4-L in $CDCl_3$.

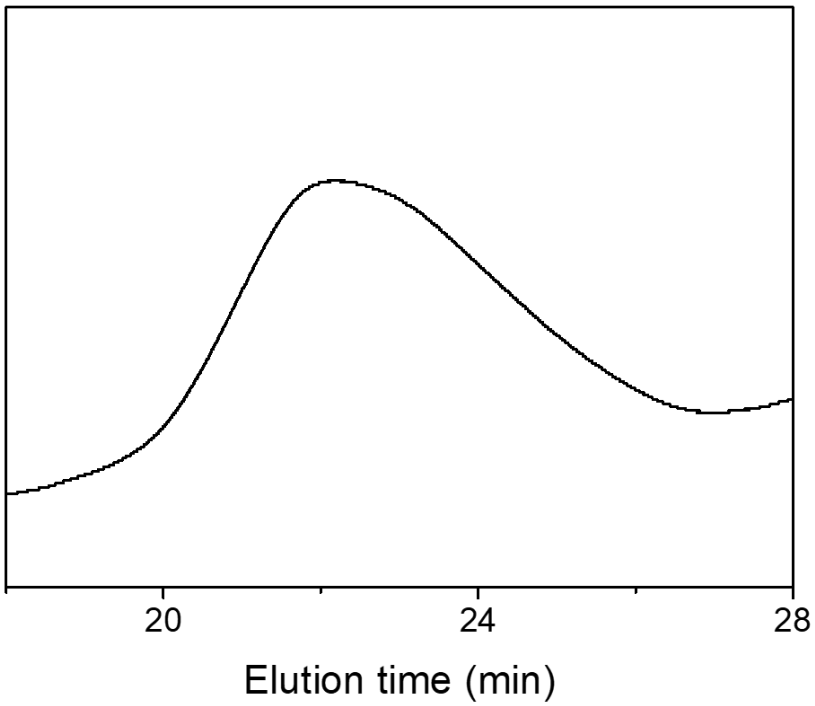

Figure S27. GPC spectra of P4-L.

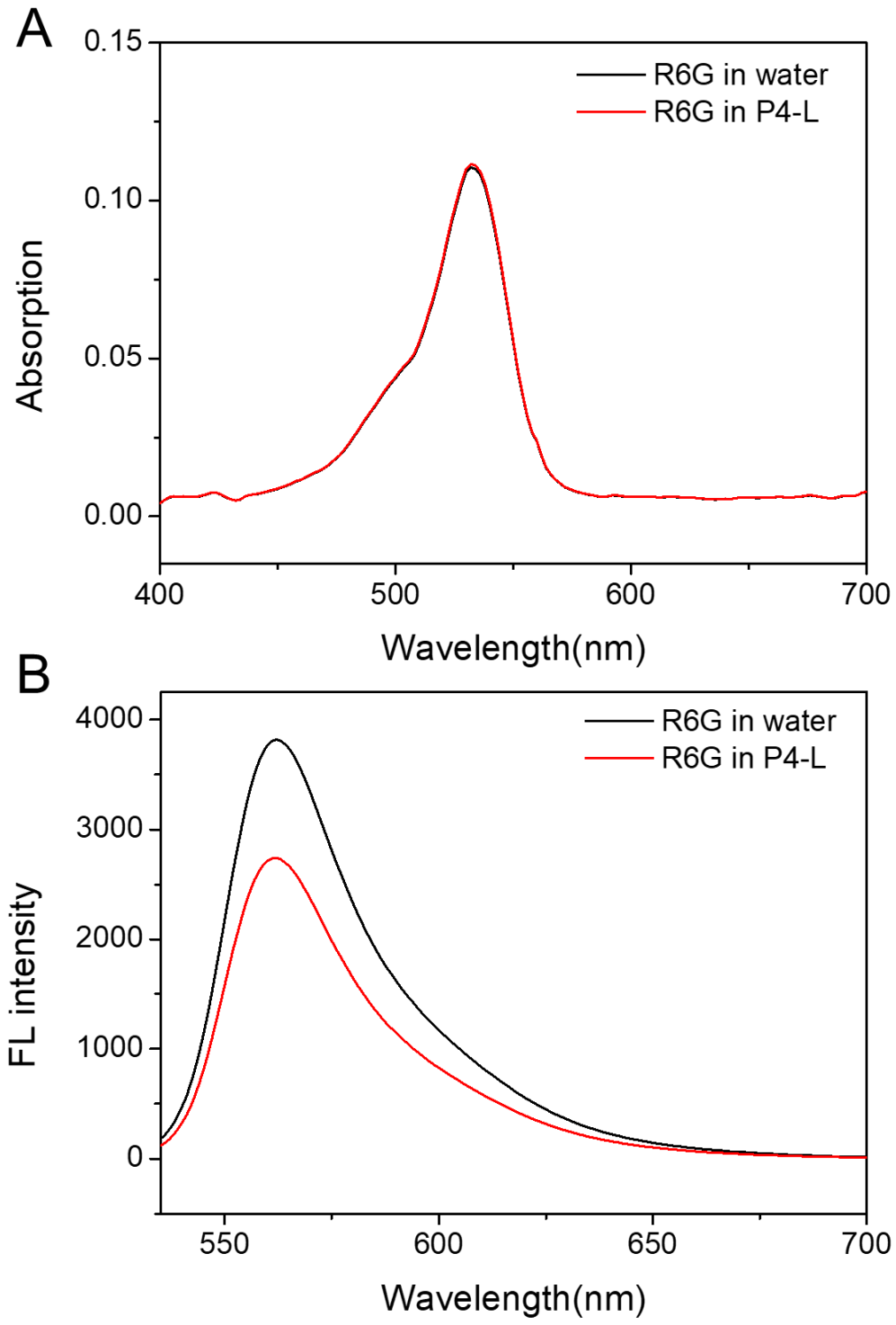

Figure S28. UV-vis spectra (A) and fluorescence emission spectra (λ_{ex} = 526 nm) (B) of R6G in water or P4-L assemblies.

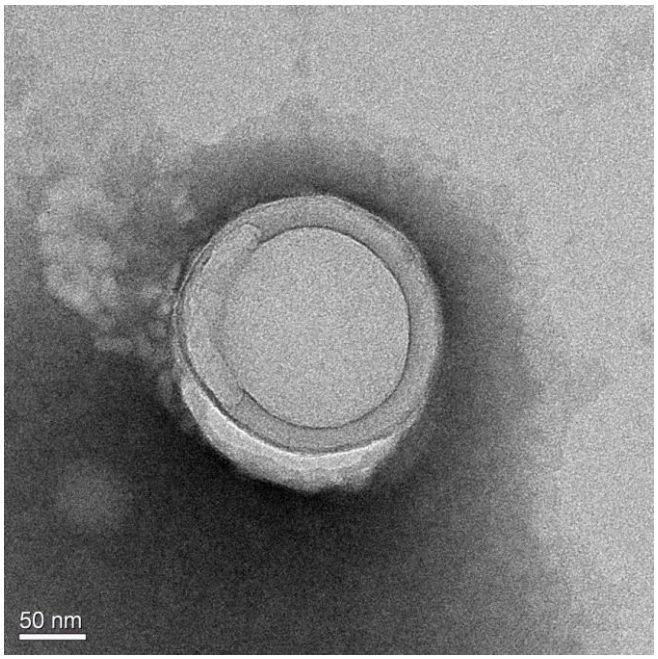

Figure S29. TEM images of P4-L. The bar is 50 nm.

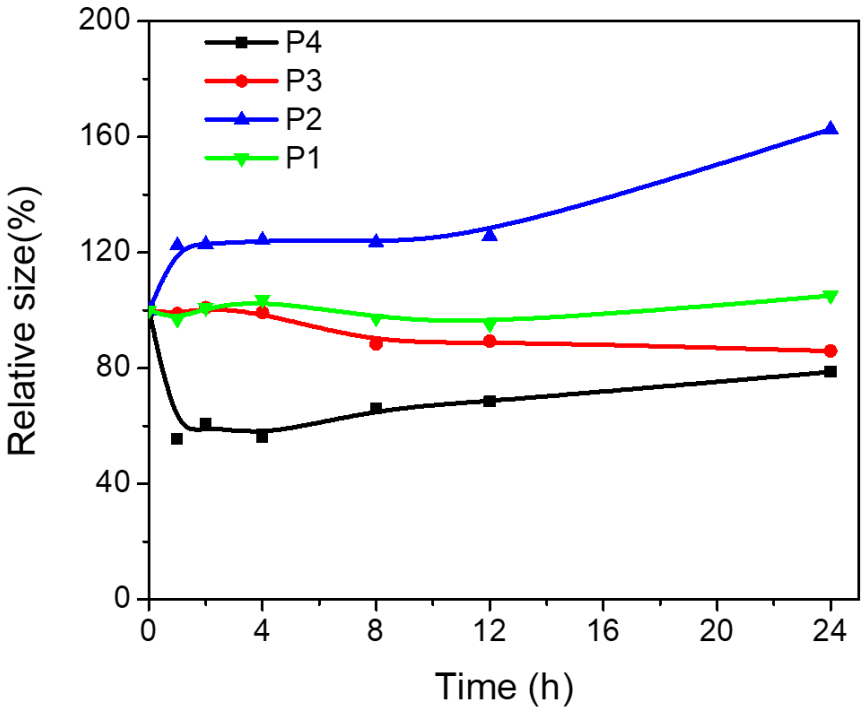

Figure S30. Change in sizes of P1, P2, P3 and P4 assemblies in response to 10 mM GSH. Relative size = S / S_0 × 100%, where S is the size of multiblock copolymer assemblies incubated with 10 mM GSH for different times, and S_0 is the original size of multiblock copolymer assemblies before treatment.

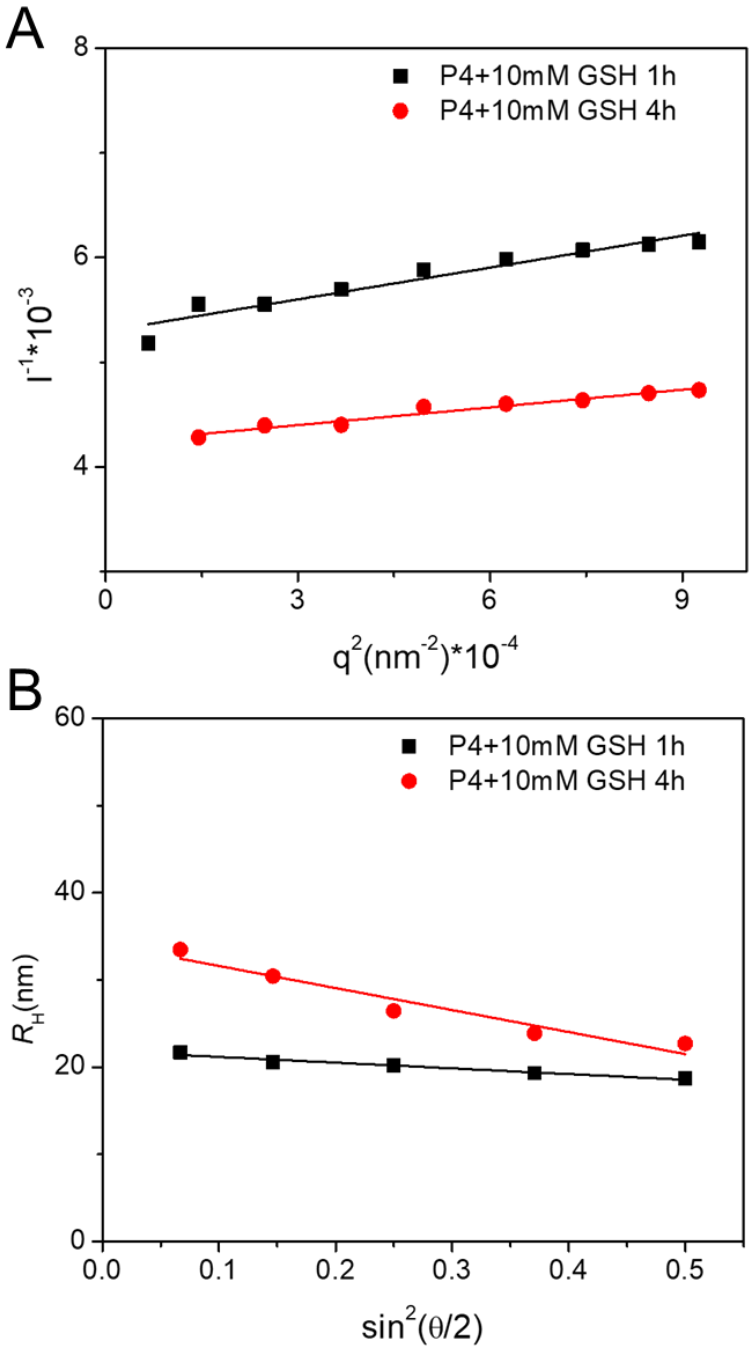

Figure S31. (A) Typical Berry plots of P4 assemblies incubated with 10 mM GSH for different times monitored at 25 °C using multi-angle SLS. (B) Hydrodynamic diameter associated functions at different incident angles for P4 assemblies incubated with 10 mM GSH for different times. The sizes, R_G and R_H values were listed in Table S 3.

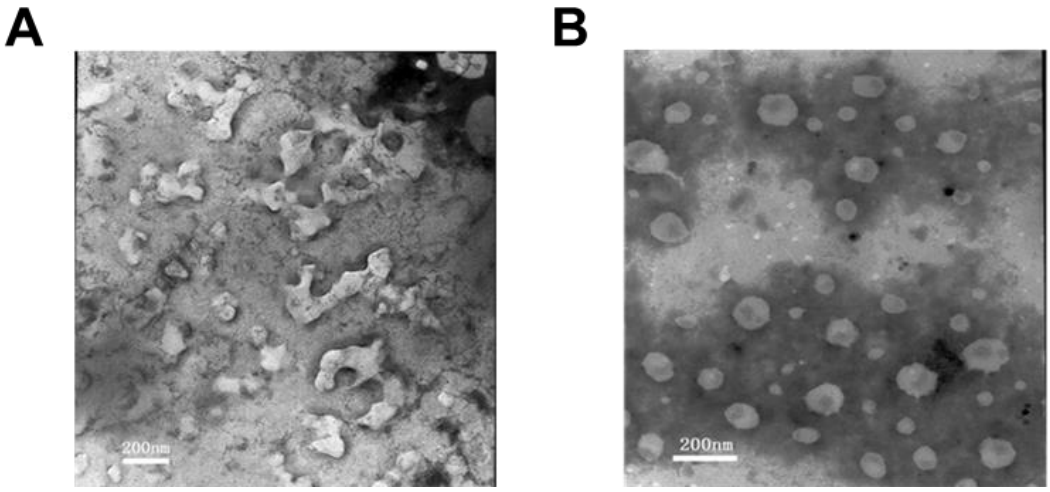

Figure S32. TEM images of P4 assemblies incubated with 10 mM GSH for 1 h (A) and 4 h (B). The bars are 200 nm.

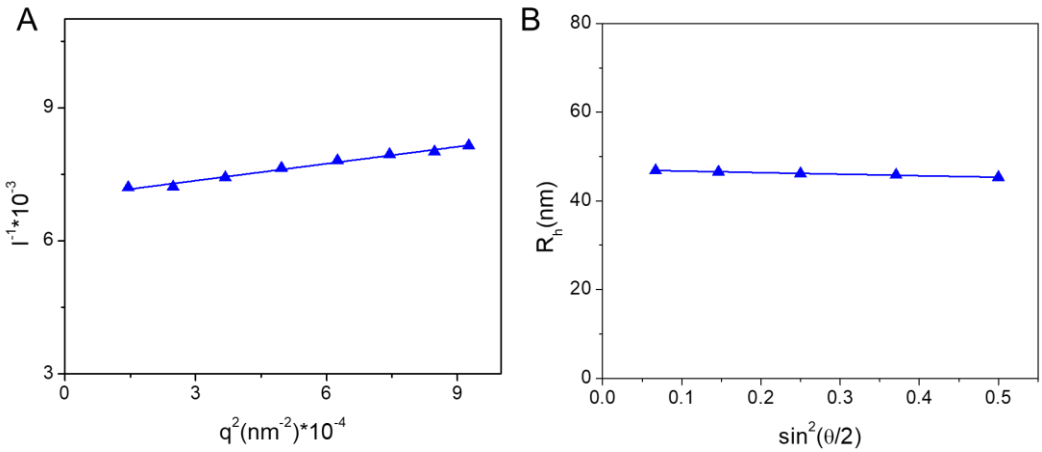

Figure S33. (A) Typical Berry plots of P3 assemblies incubated with 10 mM GSH for 4 h monitored at 25 °C using multi-angle SLS. (B) Hydrodynamic diameter associated functions at different incident angles for P3 assemblies incubated with 10 mM GSH for 4 h. The sizes, R_G and R_H values were listed in Table S3.

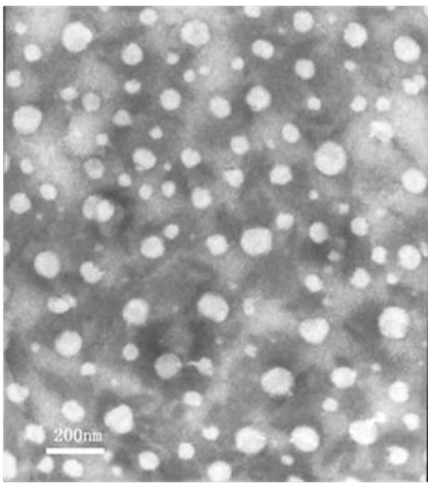

Figure S34. TEM image of P3 assemblies incubated with 10 mM GSH for 4 h. The bar is 200 nm.

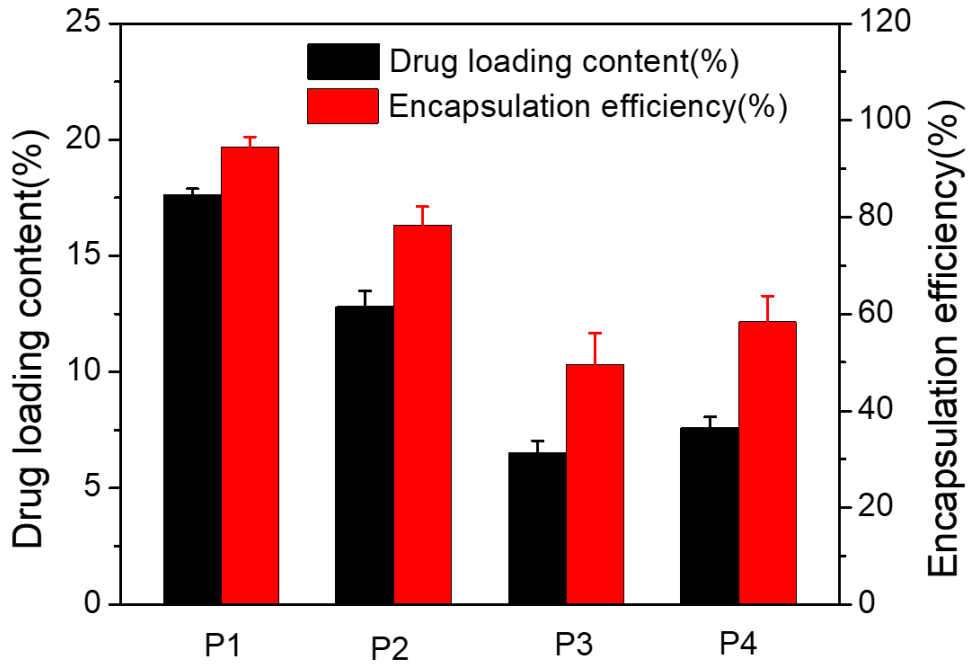

Figure S35. Loading content and encapsulation efficiency of DOX loaded in multiblock polymer assemblies.

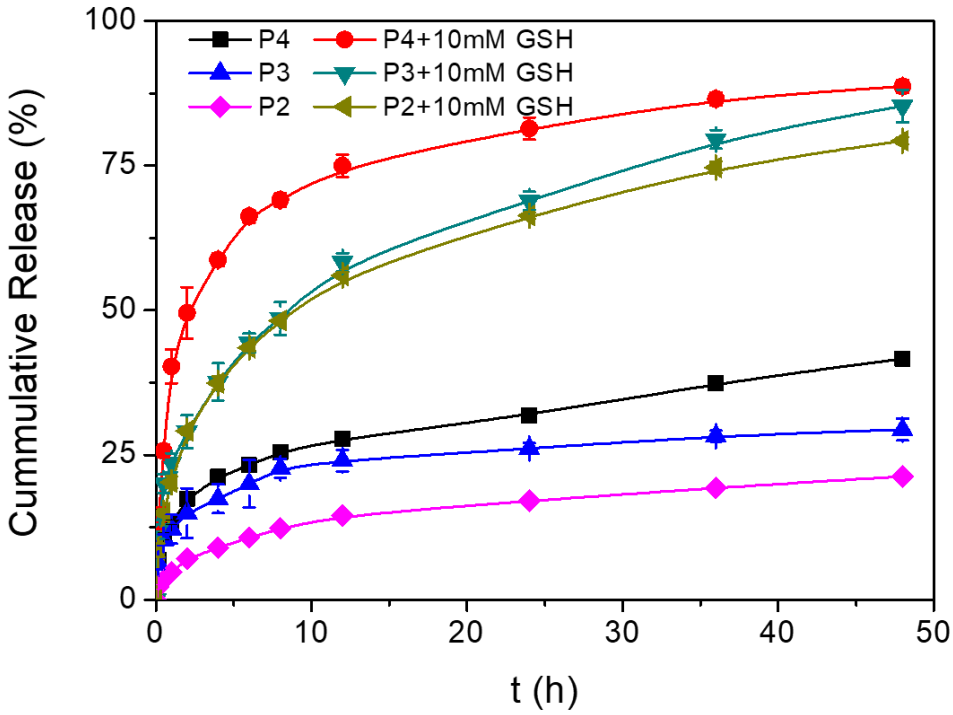

Figure S36. In vitro DOX release profiles of DOX-loaded MBC assemblies in PBS buffer (pH 7.4) with or without 10 mM GSH.

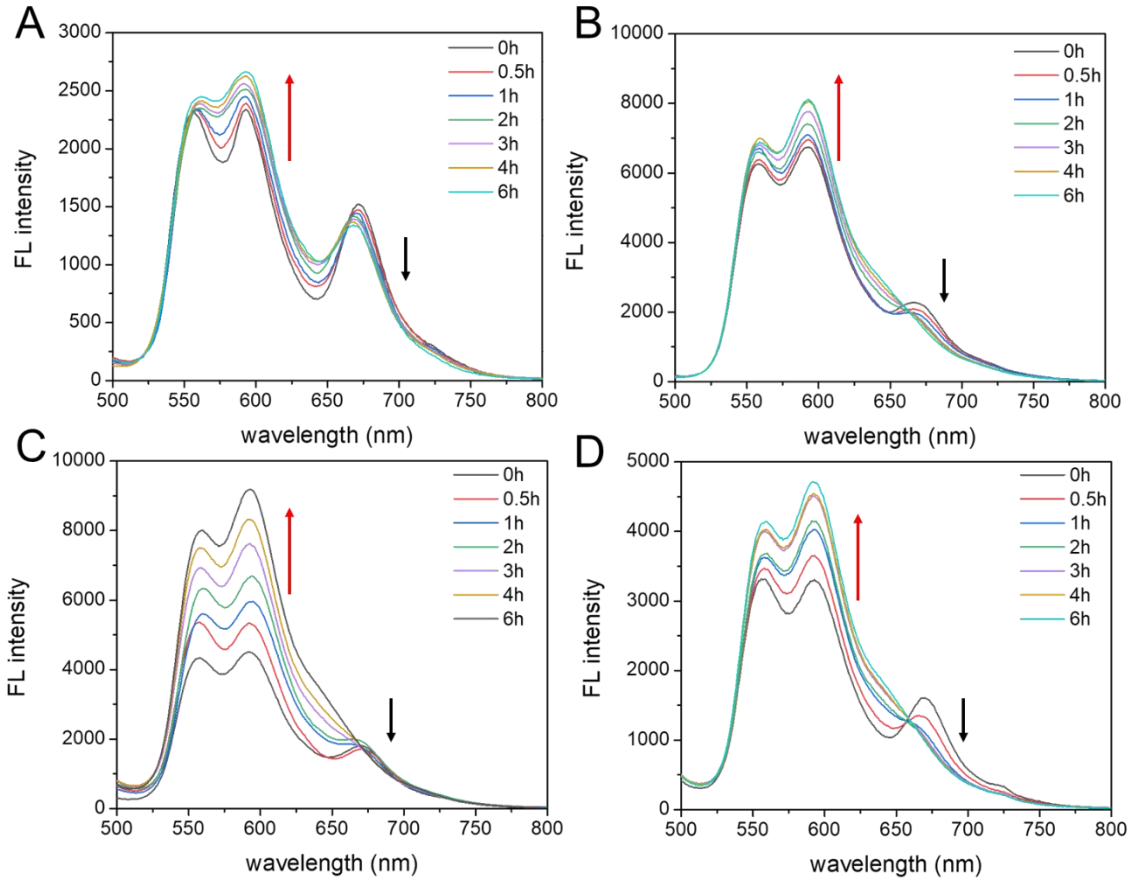

Figure S37. Fluorescence emission spectra (λ_{ex} =480 nm) of (A) DOX+Cy5@P1, (B) DOX+Cy5@P2, (C) DOX+Cy5@P3 and (D) DOX+Cy5@P4 incubated with 10 mM GSH for different times.

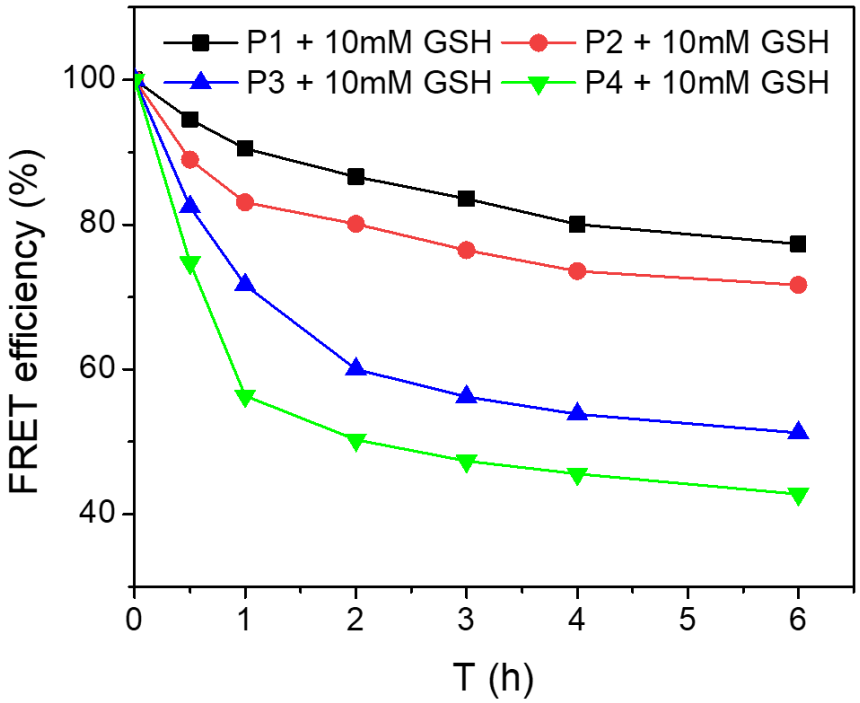

Figure S38. Normalized FRET efficiency of DOX/Cy5 encapsulated in MBC self-assemblies in the presence of 10 mM GSH.

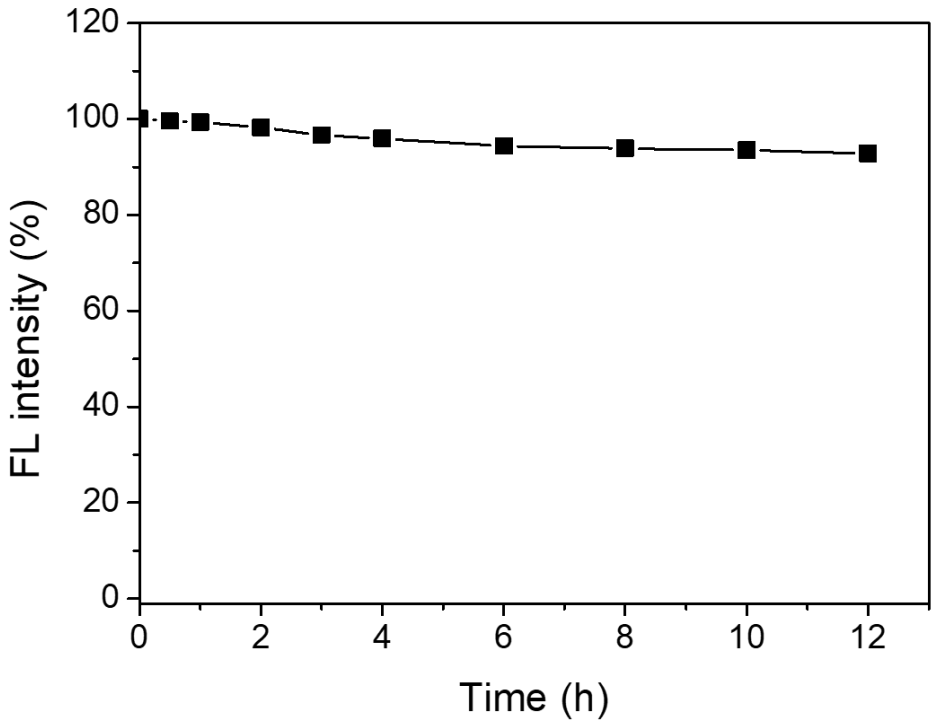

Figure S39. Normalized fluorescence intensity against time for NR-loaded P4-L assemblies in the presence of 10 mM GSH.

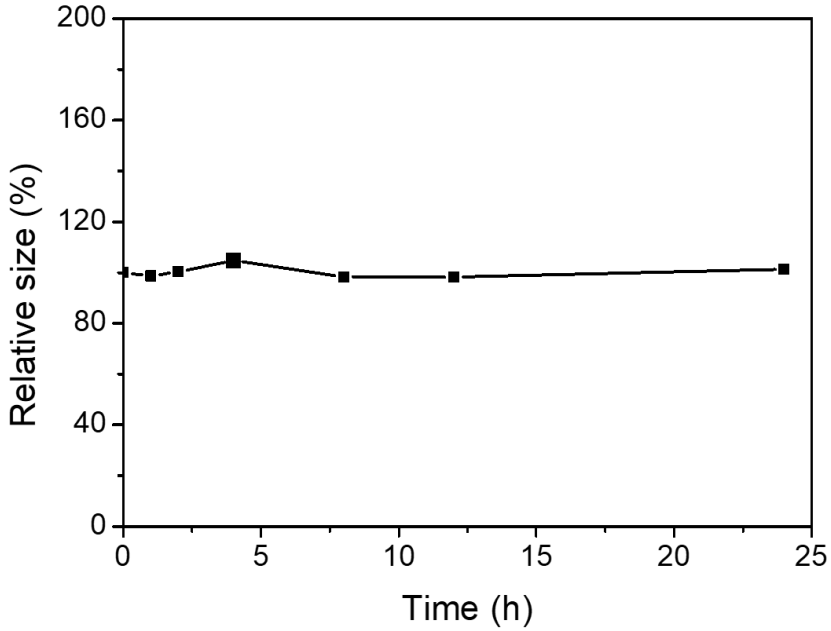

Figure S40. Change in sizes of P4-L assemblies treated with 10 mM GSH. Relative size = S / S_0 × 100%, where S is the size of P4-L assemblies incubated with 10 mM GSH for different times, and S_0 is the original size of P4-L assemblies before treatment.

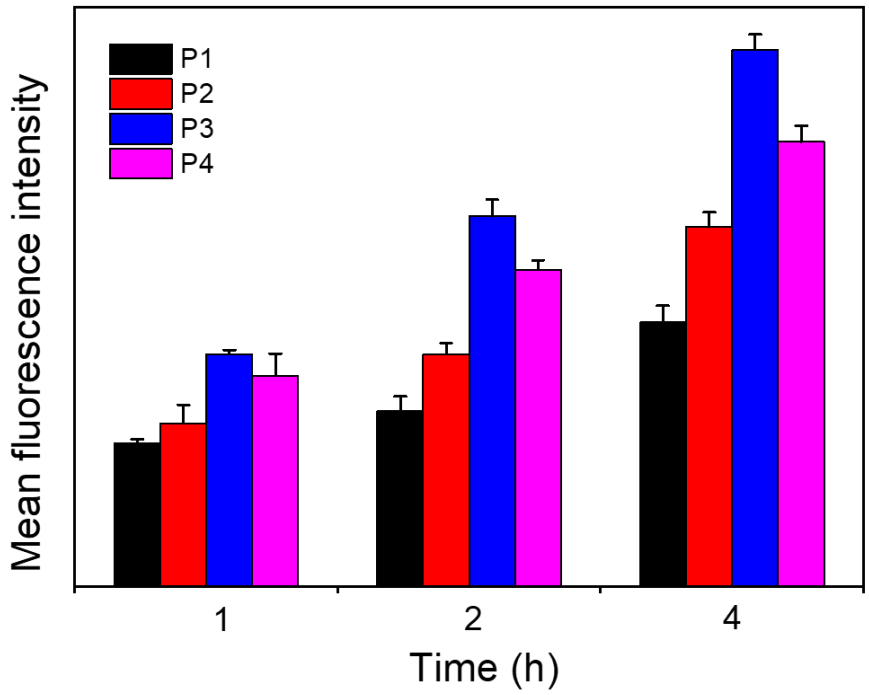

Figure S41. Flow cytometry histograms of MCF-7 tumor cells incubated with multiblock copolymer assemblies. The cells were pre-treated with BSO for 12 h.

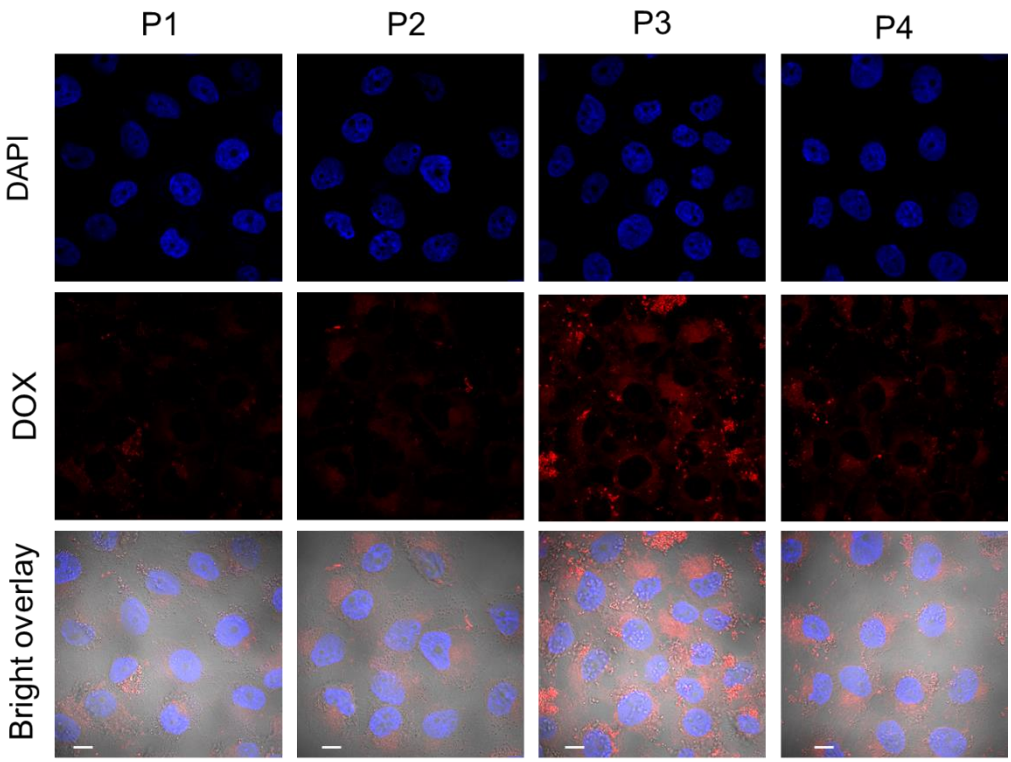

Figure S42. CLSM images of MCF-7 tumor cells incubated with various multiblock polymeric assemblies for 4 h. The cells were pre-treated with BSO for 12 h. Nuclei of cells were stained with DAPI.

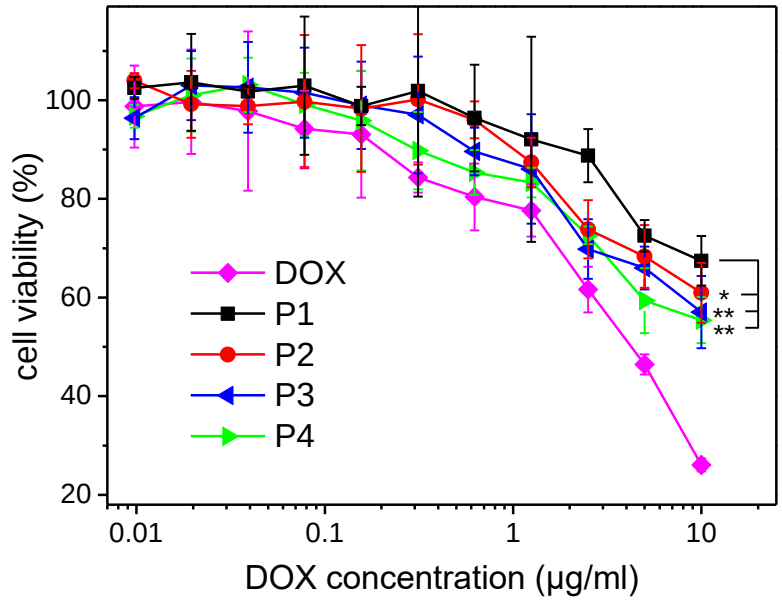

Figure S43. Cytotoxicity of DOX-loaded multiblock polymer assemblies against MCF-7 cancer cells for 24 h of incubation. Free DOX was used as a positive control.

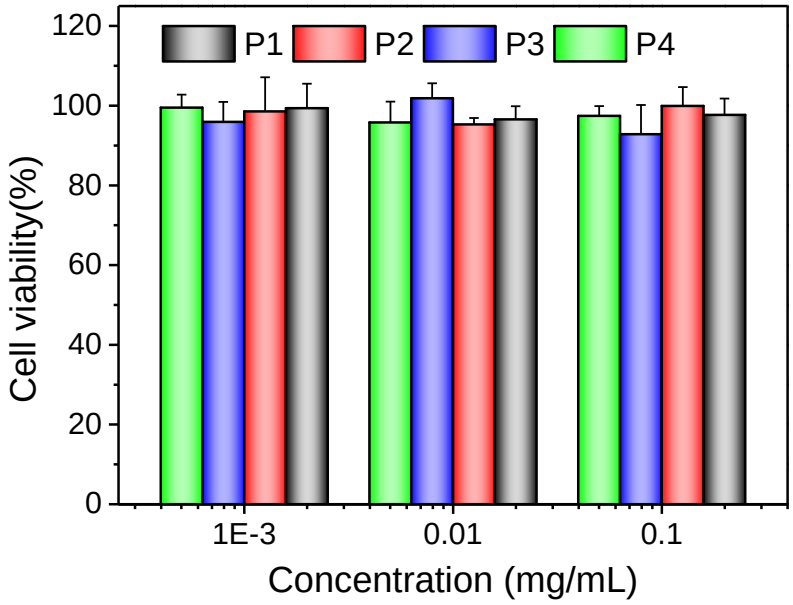

Figure S44. Cytotoxicity of drug-free polymeric assemblies against L929 fibroblasts at different concentrations.

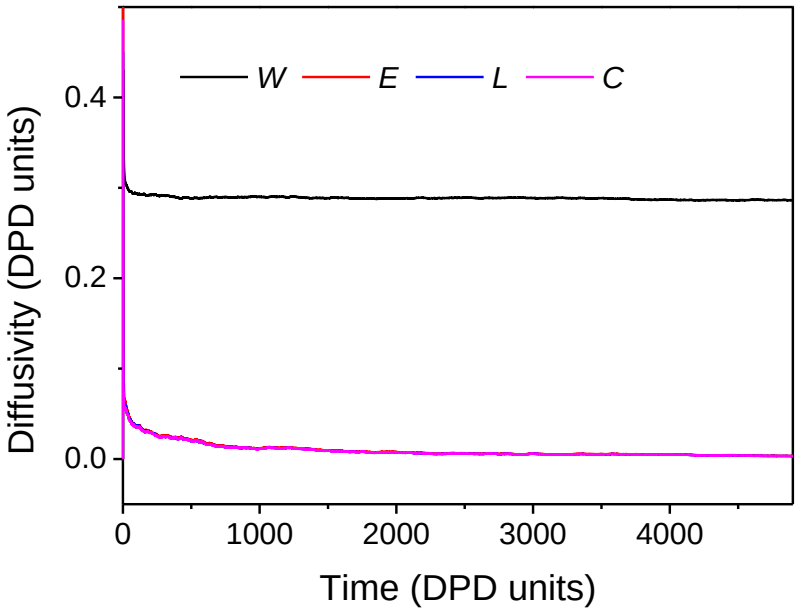

Figure S45. Evolution of the diffusion coefficient of water and multiblock copolymers against the simulation steps.

Table S1. The half inhibitory concentration (IC_{50}) of DOX-loaded multiblock polymeric self-assemblies.

Samples	DOX	P4	P3	P2	P1
IC_{50} (μg mL^{-1})	4.3	10.3	12.2	14.6	18.9

Table S2. Lifetime data for R6G dissolved in water and that encapsulated in multiblock copolymers assemblies.

Samples	τ_1(ns)	A_1(%)	τ_2(ns)	A_2(%)	τ_{av}(ns)	χ^2
water	3.921	100	--	--	3.921	0.977
P2	4.104	100	--	--	4.104	1.016
P3	4.140	100	--	--	4.140	1.053
P4	1.009	20	3.929	80	3.340	1.005

Table S3. DLS and SLS data of P4 and P3 assemblies incubated with 10 mM GSH for different times.

Samples	Time (h)	Size (nm)	R_H (nm)	R_G (nm)	R_G/R_H
P4	1	91.9	21.9	33.9	1.6
P4	4	92.8	47.1	33.1	0.70
P3	4	102	48.4	36.1	0.75

Supporting References

S1 A. J. Adler, N. J. Greenfield, G. D. Fasman, *Method Enzymol.* **1973**, *27*, 675.

S2 N. J. Greenfield, *Nat. Protoc.* **2006**, *1*, 2876.

S3 M. van der Schuur, B. Noordover, R. J. Gaymans, *Polymer* **2006**, *47*, 1091.

S4 H. Tan, J. Li, M. Guo, R. Du, X. Xie, Y. Zhong, Q. Fu, *Polymer* **2005**, *46*, 7230.

S5 A. Marcos-Fernández, G. A. Abraham, J. L. Valentín, J. S. Román, *Polymer* **2006**, *47*, 785.

S6 X. J. Loh, K. B. Colin Sng, J. Li, *Biomaterials* **2008**, *29*, 3185.

S7 J. Guan, M. S. Sacks, E. J. Beckman, W. R. Wagner, *J. Biomed. Mater. Res.* **2002**, *61*, 493.

S8 I. Yilgor, E. Yilgor, S. Das, G. L. Wilkes, *J. Polym. Sci. Pol. Phys.* **2009**, *47*, 471.

S9 M. Wilhelm, C. Zhao, Y. Wang, R. Xu, M. A. Winnik, *Macromolecules* **1991**, *24*, 1033.

S10 I. Astafieva, X. F. Zhong, A. Eisenberg, *Macromolecules* **1993**, *26*, 7339.

S11 C. Kim, X. Hu, S. Park, *J. Am. Chem. Soc.* **2016**, *138*, 14941.

S12 A. L. Plant, *Photochem. Photobiol.* **1986**, *44*, 453.

S13 D. Fuhrmann, T. Benzler, S. Fernando, T. Endres, T. Dreier, S. A. Kaiser, C. Schulz, *P. Combust. Inst.* **2017**, *36*, 4505.

S14 M. Fedoseeva, R. Letrun, E. Vauthey, *J. Phys. Chem. B* **2014**, *118*, 5184.

S15 P. Y. Chen, D. Pearce, A. S. Verkman, *Biochemistry* **1988**, *27*, 5713.

S16 A. Harada, S. Cammas, K. Kataoka, *Macromolecules* **1996**, *29*, 6183.

S17 T. Mondal, K. Dan, J. Deb, S. S. Jana, S. Ghosh, *Langmuir* **2013**, *29*, 6746.

S18 P. J. Hoogerbrugge, J. M. V. A. Koelman, *Europhys. Lett.* **1992**, *19*, 155.

S19 P. Español, P. Warren, *Europhys. Lett.* **1995**, *30*, 191.

S20 X. D. Guo, J. P. K. Tan, S. H. Kim, L. J. Zhang, Y. Zhang, J. L. Hedrick, Y. Y. Yang, Y. Qian,

Biomaterials **2009**, *30*, 6556.

S21 R. D. Groot, P. B. Warren, *J. Chem. Phys.* **1997**, *107*, 4423.

S22 Y. Lin, H. Chang, Y. Sheng, H. Tsao, *Macromolecules* **2012**, *45*, 7143.

S23 S. H. Chou, H. K. Tsao, Y. J. Sheng, *J. Chem. Phys.* **2006**, *125*, 194903.

S24 H. Tan, C. Yu, Z. Lu, Y. Zhou, D. Yan, *Soft Matter* **2017**, *13*, 6178.

S25 S. Ma, M. Xiao, R. Wang, *Langmuir* **2013**, *29*, 16010.

S26 X. Li, *Soft Matter* **2013**, *9*, 11663.

S27 Y. Lin, H. Chang, Y. Sheng, H. Tsao, *Soft Matter* **2014**, *10*, 1500.

S28 Y. Lin, H. Chang, Y. Sheng, H. Tsao, *Soft Matter* **2014**, *10*, 1840.

S29 Y. Lin, H. Chang, Y. Sheng, H. Tsao, *Soft Matter* **2013**, *9*, 4802.

S30 N. Arai, K. Yasuoka, X. C. Zeng, *ACS Nano* **2016**, *10*, 8026.

S31 R. D. Groot, K. L. Rabone, *Biophys. J.* **2001**, *81*, 725.

S32 S. Saeki, N. Kuwahara, M. Nakata, M. Kaneko, *Polymer* **1976**, *17*, 685.